NATIONAL ENERGY TECHNOLOGY LABORATORY

Experimental and Simulation Analysis of Binary Mixtures of Biomass and Inert Material

18 May 2020

U.S. DEPARTMENT OF ENERGY | NATIONAL ENERGY TECHNOLOGY LABORATORY

Office of Fossil Energy

DOE/NETL-2020/2134

Disclaimer

This work was funded by the Department of Energy, National Energy Technology Laboratory, an agency of the United States Government, through a support contract with Leidos Research Support Team (LRST).

Cover Illustration: Snapshots from the experiments with large size biomass and glass beads showing slugging at lower fluidization velocities and good mixing at higher fluidization velocities.

Suggested Citation: Chandramouli, D.; Ashfaq, H.; Rogers, W. A. *Experimental and Simulation Analysis of Binary Mixtures of Biomass and Inert Material*; DOE/NETL-2020/2134; NETL Technical Report Series; U.S. Department of Energy, National Energy Technology Laboratory: Morgantown, WV, 2020; p. 44. DOI: 10.2172/1619201.

An electronic version of this report can be found at: https://netl.doe.gov/TRS

Experimental and Simulation Analysis of Binary Mixtures of Biomass and Inert Material

Deepthi Chandramouli[1,2], Huda Ashfaq[3], William A. Rogers[1]

[1] U.S. Department of Energy, National Energy Technology Laboratory, 3610 Collins Ferry Road, Morgantown, WV 26507

[2] U.S. Department of Energy, National Energy Technology Laboratory, Leidos Research Support Team, 3610 Collins Ferry Road, Morgantown, WV 26507

[3] U.S. Department of Energy, National Energy Technology Laboratory, Oak Ridge Institute for Science and Education, 3610 Collins Ferry Road, Morgantown, WV 26507

DOE/NETL-2020/2134

18 May 2020

NETL Contacts:

William A. Rogers, Principal Investigator

Jonathan Lekse, Technical Portfolio Lead

Bryan Morreale, Executive Director, Research & Innovation Center

This page intentionally left blank.

Table of Contents

ABSTRACT **1**
1. INTRODUCTION **2**
2. EXPERIMENTAL SET-UP **4**
2.1 LABORATORY TEST PROCEDURE 4
2.2 PREPARATION OF THE BIOMASS SAMPLES 5
2.3 EXPERIMENTAL PROCEDURE 8
3. EXPERIMENTAL RESULTS **11**
4. SIMULATION SET-UP AND RESULTS **15**
4.1 THE HYBRID DRAG MODEL 15
4.2 RESULTS 16
5. CONCLUSIONS AND FUTURE WORK **29**
6. REFERENCES **30**
APPENDIX **A-1**

This page intentionally left blank.

List of Figures

Figure 1: Schematic of the test rig. 4
Figure 2: Photomicrograph of the biomass sample: size range 1 - small. 5
Figure 3: Photomicrograph of the biomass sample: size range 2 – medium. 6
Figure 4: Photomicrograph of the biomass sample: size range 3 – large. 6
Figure 5: Particle size distribution of the biomass – size range 1 – termed "small". 7
Figure 6: Particle size distribution of the biomass – size range 2 – termed "medium" 7
Figure 7: Particle size distribution of the biomass – size range 3 – termed "large" 8
Figure 8: Variation of the inlet gas flow rate (velocity) during the laboratory fluidization tests. . 9
Figure 9: Snapshots from experiment – mixture of glass beads and 4 g of large-sized biomass: (a) 1 U_{mf}, and (b) 2 U_{mf} 11
Figure 10: Snapshots from the experiment – 4 g of large size biomass: (a) 3 U_{mf}, (b) 4 U_{mf}, and (c) 5 U_{mf}. 12
Figure 11: Snapshots from the experiment – 2 g of large size biomass: (a) 3 U_{mf}, (b) 4 U_{mf}, and (c) 5 U_{mf}. 12
Figure 12: Snapshots from the experiment – 4 g of medium size biomass: (a) 1 U_{mf}, and (b) 2 U_{mf}. 13
Figure 13: Snapshots from the experiment – 4 g of medium size biomass: (a) 3 U_{mf}, (b) 4 U_{mf}, and (c) 5 U_{mf} 13
Figure 14: Pressure drop (Pa) for different mass loadings of the small size biomass at a gas velocity of 3 U_{mf}. 14
Figure 15: Comparison of the pressure drops for the small size biomass (2 g) – experiments vs. DEM simulations. 18
Figure 16: Comparison of the pressure drops for the small size biomass (4 g) – experiments vs. DEM simulations. 19
Figure 17: Comparison of the pressure drops for the small size biomass (6 g) – experiments vs. DEM simulations. 20
Figure 18: Comparison of the pressure drops for the medium size biomass (2 g) – experiments vs. DEM simulations 21
Figure 19: Comparison of the pressure drops for the medium size biomass (4 g) – experiments vs. DEM simulations 22
Figure 20: Comparison of the pressure drops for the medium size biomass (6 g) – experiments vs. DEM simulations 23
Figure 21: Comparison of the pressure drops for the large size biomass (2 g) – experiments vs. DEM simulations. 24
Figure 22: Comparison of the pressure drops for the large size biomass (4 g) – experiments vs. DEM simulations. 25
Figure 23: Comparison of a snapshot from the experiment (left) and the simulation (right) for the large biomass mixture (4 g) at 5 U_{mf}. 26
Figure 24: Comparison of a snapshot from the experiment (left) and the simulation (right) for the medium biomass mixture 27
Figure 25: Comparison of a snapshot from the experiment (left) and the simulation (right) for the small biomass mixture 28

List of Tables

Table 1: Test Matrix 8

Acronyms, Abbreviations, and Symbols

Term	Description
BETO	Bioenergy Technologies Office
CFB	Circulating fluidized bed
DEM	Discrete element method
MFAL	Multiphase Flow Analysis Laboratory
MFiX	Multiphase Flow with Interphase eXchanges
SMD	Sauter mean diameter
U_{mf}	Minimum fluidization velocity

This page intentionally left blank.

Acknowledgments

This work was performed in support of the U.S. Department of Energy's (DOE) Bioenergy Technologies Office Research Program. The research was executed through the National Energy Technology Laboratory's (NETL) Research and Innovation Center's Consortium for Computational Physics and Chemistry - Biopower Field Work Proposal. Research performed by Leidos Research Support Team staff was conducted under the RSS contract 89243318CFE000003.

The authors would like to thank Rupendranath Panday and Jia Yu for their assistance with the laboratory tests, and Liqiang Lu for his guidance with the simulation effort.

This page intentionally left blank.

ABSTRACT

A literature review was conducted to identify experiments on various scales of biomass combustion specific to circulating fluidized bed (CFB) combustors. Typical feedstock and inert bed material characteristics for biomass combustion in a CFB were gathered. This information was used to design laboratory-scale, non-reacting experiments on biomass-inert bed material mixtures in a 1-in. cylindrical test rig in the Multiphase Flow Analysis Laboratory (MFAL) in Morgantown, WV. The biomass chosen was a hardwood. Pellets from the hardwood were milled and sieved to obtain three size ranges—small, medium, and large. Three mass loadings of each of the biomass samples were fluidized with glass beads as the inert bed material to study the mixing characteristics under varying fluidizing gas velocities. Hydrodynamic data including pressure drop measurements at select vertical locations and video recordings of the mixture behavior were generated in this effort. The data was used to guide development of suitable drag models and associated parameters and to validate the model performance quantitively as well as qualitatively. Future plans include coupling the validated drag model with kinetic schemes identified for biomass pyrolysis and combustion to perform laboratory scale and commercial scale reactor modeling.

1. INTRODUCTION

Biomass combustion in fluidized beds is an efficient method for power generation because of the ability to control the emissions of pollutants. Wood is a very popular fuel selected for such applications. Fluidization of wood is challenging; therefore, an inert bed material is used for fluidized bed applications with wood. Capturing the hydrodynamics of the wood—inert bed material mixture is crucial as it impacts the heat transfer between the two phases as well as with the gas phase which impact the effectiveness of the physical process being modeled.

Assessment of the drag model appropriate for such binary mixtures marks the first step in reactor-scale modeling. To enable validation, cold-flow laboratory-scale experiments were performed to collect data on biomass-inert material mixtures at different operating conditions. The open-source software Multiphase Flow with Interphase eXchanges (MFiX-DEM, discrete element model) application was used to model the system. The goal of this effort is to identify a drag model that is most suited for modeling fluidization behavior of such mixtures.

A literature survey was conducted to identify different scales of biomass combustion in circulating fluidized-bed combustors. The study focused on feedstocks like red oak, corn stover lignin, and municipal solid waste feeds, which are of interest to the Bioenergy Technologies Office (BETO) biopower project. The feedstock and inert bed material characteristics from these references were used to design the lab-scale experiments. Desroches-Ducarne et al. (1998) studied the co-combustion of coal and municipal solid waste in a circulating fluidizing bed (CFB) with biomass mass ratio varying from 0 to 1. Their results were based on a 25 kW unit, with a 10-cm inner diameter and 4-m tall riser. Their bed material comprised of 0.2 mm sand and the feedstock was dried and ground to obtain a mean diameter of 0.5 mm. They reported the measurements of the combustion product gas composition varying with different mass fractions of biomass—coal mixtures. Knobig et al. (1998) compared a small laboratory-scale CFB combustor (height 16 m, inner diameter 100 mm) and a large-scale combustor 12 MWth (height 14 m, cross-sectional dimensions of 1.6 m x 1.6 m) with respect to pollutant formation and reduction for different fuels. The particle size of fuels used was similar in both cases having diameter <9 mm. They reported gas concentration values for CO, O_2, NO, and N_2O as a function of axial height for both types of combustors.

Youssef et al. (2009) performed an experimental study on the combustion of four types of biomass—sawdust wood, wheat straw, corncobs, and cottonseed burs, each of them at three excess air ratios (excess air ratio is defined as actual air-to-fuel ratio divided by the theoretical air-to-fuel ratio)—1.08, 1.24, and 1.4 in a circulating fluidized bed. Their apparatus consisted of a 145-mm inner diameter steel cylinder, 2-m tall, with measurements of temperature along the axial height and the gas (CO and NOx) emissions measured at the outlet. Their results indicated that excess air ratio had no dependence on temperature distribution; however, CO emissions were lowest at an excess air ratio of 1.24.

Leckner and Karlsson (1993) studied the emissions of NO, N_2O, CO, and SO_2 during combustion of wood in a CFB boiler. The experiments were performed in a 12 MW CFB boiler at Chalmers University. The rectangular combustion chamber had dimensions of 1.7-m wide x 1.7-m deep x 13.5-m high. The inert bed material was sand with a mean diameter of 0.35 mm and the fuels used were sawdust, birch chips, fir chips, and coal. The size of sawdust particles was less than 8 mm, the size of the birch and fir chips were about 1–3 mm thick and 5–45 mm in length. They reported values of nitric oxide concentrations with varying bed temperatures,

fluidization velocities nitrogen quantity in the fuel (birch chips have higher amount of nitrogen than fir chips). They concluded that fuel nitrogen is the most important parameter affecting NO emissions, and biomass NO emissions were generally lower than NO emissions from coal. Lyngfelt and Leckner (1999) studied the combustion of wood chips in the same boiler as above, varying the temperature and air-staging (primary – secondary air). They reported measurements of emissions of CO and NO as functions of exit chamber temperature and air ratios.

Belin et al. (1988) provided the boiler design and fuel/bed material data for commercial-scale fluidized bed boilers with capacities of 25 MWe and 16 MWe. The furnace had a rectangular cross section and sand was used as the inert bed material. The feedstock was comprised of two sets of wood chips in different size ranges, one in the size range < 50 mm (predominantly coarse particles) and the other in the size range < 13 mm (predominantly fine particles). The influence of fuel properties (moisture content, particle size, composition, and reactivity) on biomass combustion was analyzed. They published data on the furnace temperature and gas concentration patterns as a function of fuel properties, combustion air distribution, and solids circulation. Carbon conversion and CO/NOx emissions data are also presented.

Cui et al. (2007) reviewed the work on hydrodynamics and mixing of biomass particles in fluidized beds. They summarized their findings on terminal setting velocities, minimum fluidization and fluidizability of biomass mixtures, primarily for lower velocity fluidization. They also presented discussions about mixing and solids circulation and gas–solids mixing in circulating fluidized beds. Gungor (2008) and Gungor and Eskin (2007) performed two-dimensional modeling of biomass combustion in two stages—the bed hydrodynamics were validated initially and the kinetics were added later. For the hydrodynamics, the model results were validated with the data from atmospheric cold bed CFB units. The quantities of interest in the study were axial and radial distribution of void fraction, solids volume fraction and particle velocity, total pressure drop along the bed height, and radial solids flux. A broad range of experimental data were considered as follows: bed diameter from 0.05–0.418 m, bed height from 5–18 m, mean particle diameter from 67–520 μm, particle density from 1,398 to 2,620 kg/m^3, mass fluxes from 21.3 to 300 kg/m^{2}s and gas superficial velocities from 2.52–9.1 m/s. Adanez et al. (2003) modeled the combustion of wood chips in a CFB combustor. They compared results of oxygen profiles, the average char concentrations, and particle sizes along the riser, using the data from the 12 MWth unit at Chalmers University. To achieve better agreement with data, they included biomass particle fragmentation in their model.

Despite growing research interest in the area of biomass combustion, experiments pertaining to detailed hydrodynamics of biomass particles in the presence of an inert bed material is limited. These are critical in understanding phase distribution and separation of mixtures. In the current study, results from the experiments and numerical simulations on fluidization of mixtures of biomass and glass particles are presented. The remainder of this report is organized as follows: In Section 2 the laboratory test set-up, procedure and some initial observations are presented followed by experimental results in Section 3. The details of the model and the simulation results are presented in Section 4. Finally, the summary and scope for future work are presented in Section 5.

2. EXPERIMENTAL SET-UP

2.1 LABORATORY TEST PROCEDURE

Based on the feedstock and bed material information obtained from the literature, laboratory-scale experiments were designed to obtain hydrodynamic interaction of the two solid phases during fluidization. The chosen specifications for the inert bed material as well as for biomass was similar to typical commercial scale systems.

The experiments were performed in a 1-in. (2.54 cm) inner diameter acrylic cylinder test rig. The rig had six pressure measurement ports in the lower region (particle bed) and one pressure measurement port at the top of the freeboard region. The pressure measurement frequency was 100 Hz and the flow rate measurement frequency was 1 Hz. A schematic of the pressure drop locations in the test rig is shown in Figure 1. Glass beads with a Sauter mean diameter (SMD) of 353 µm was used as the bed material. Crushed hardwood pellets were used as the feedstock. These were later sieved to obtain three size ranges representative of laboratory and pilot-scale systems. Three mass loadings of glass bead mixtures were chosen for the feedstock. Details are provided in the sections below.

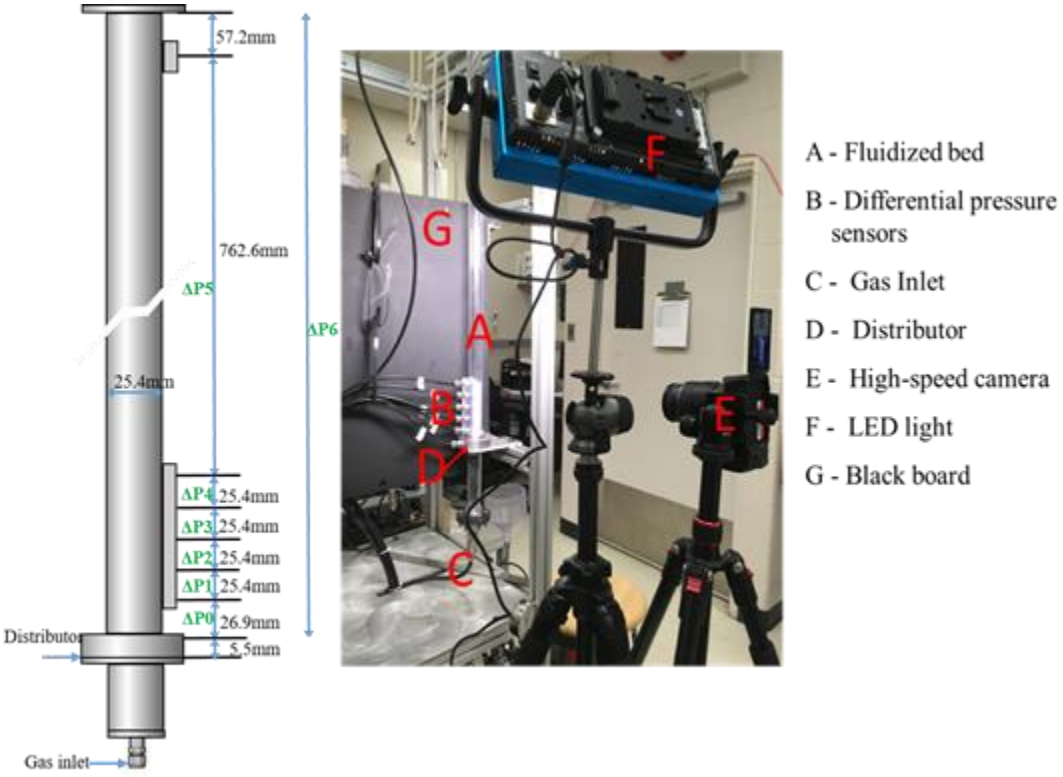

Figure 1: Schematic of the test rig.

2.2 PREPARATION OF THE BIOMASS SAMPLES

Hardwood pellets were hand milled and sieved to obtain three size ranges, as detailed below.

- Size Range 1 (Small) – SMD 332 µm: A 355 µm sieve was used to limit the maximum particle size. A 150 µm sieve was used to limit the minimum particle size.
- Size Range 2 (Medium) – SMD 699 µm: A 850 µm sieve was used to limit the maximum particle size. A 355 µm sieve was used to limit the minimum particle size.
- Size Range 3 (Large) – SMD 1,549 µm: A 1,700 µm sieve was used to limit the maximum particle size. An 850 µm sieve was used to limit the minimum particle size.

Photomicrographs of the samples are shown in Figure 2 through Figure 4.

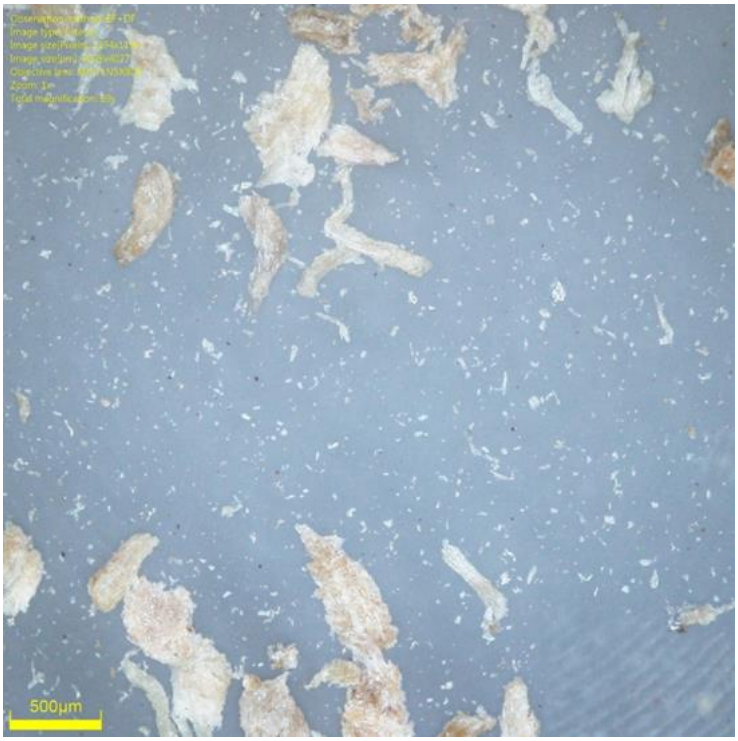

Figure 2: Photomicrograph of the biomass sample: size range 1 - small.

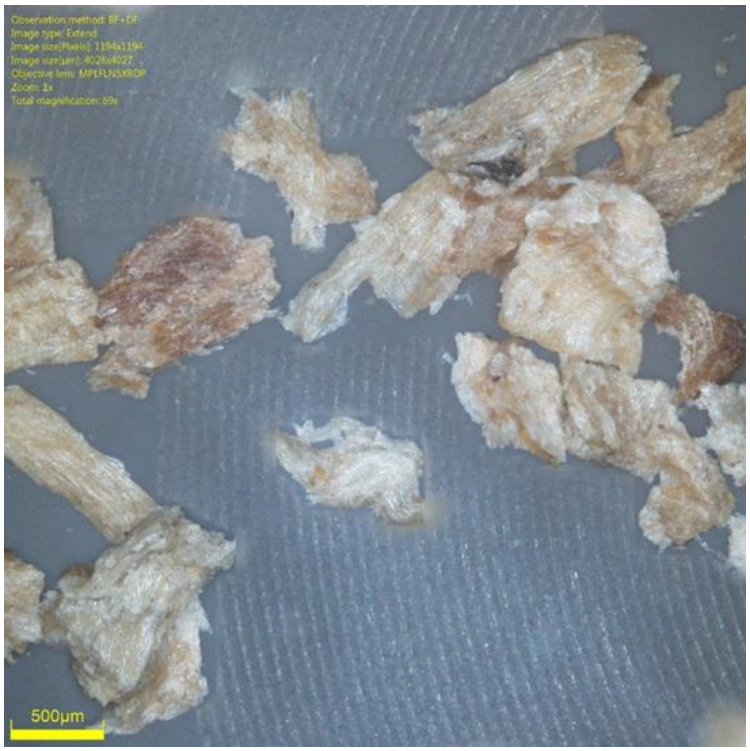

Figure 3: Photomicrograph of the biomass sample: size range 2 – medium.

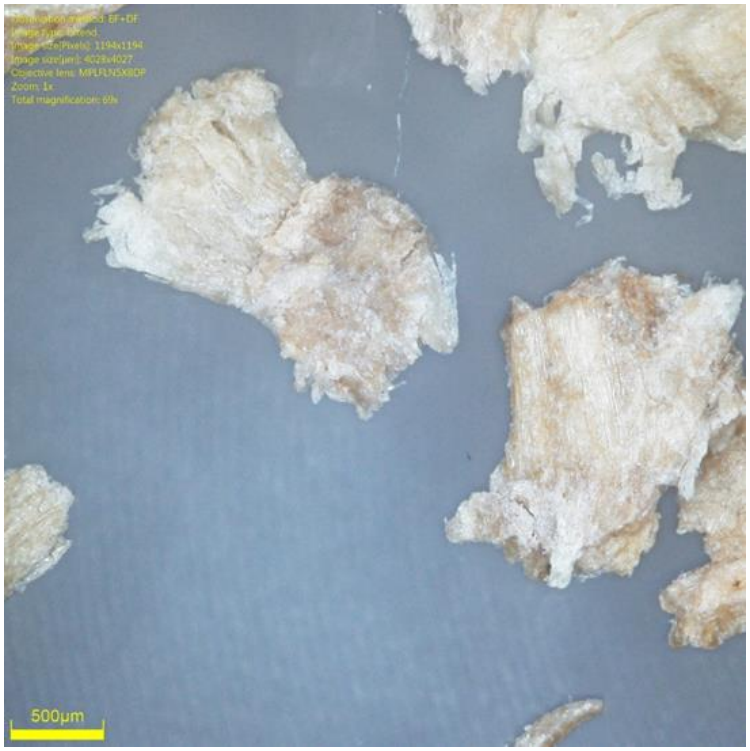

Figure 4: Photomicrograph of the biomass sample: size range 3 – large.

The particle size range of the crushed wood pellet sample was analyzed using QICPIC. The size distributions are shown in Figure 5 through Figure 7.

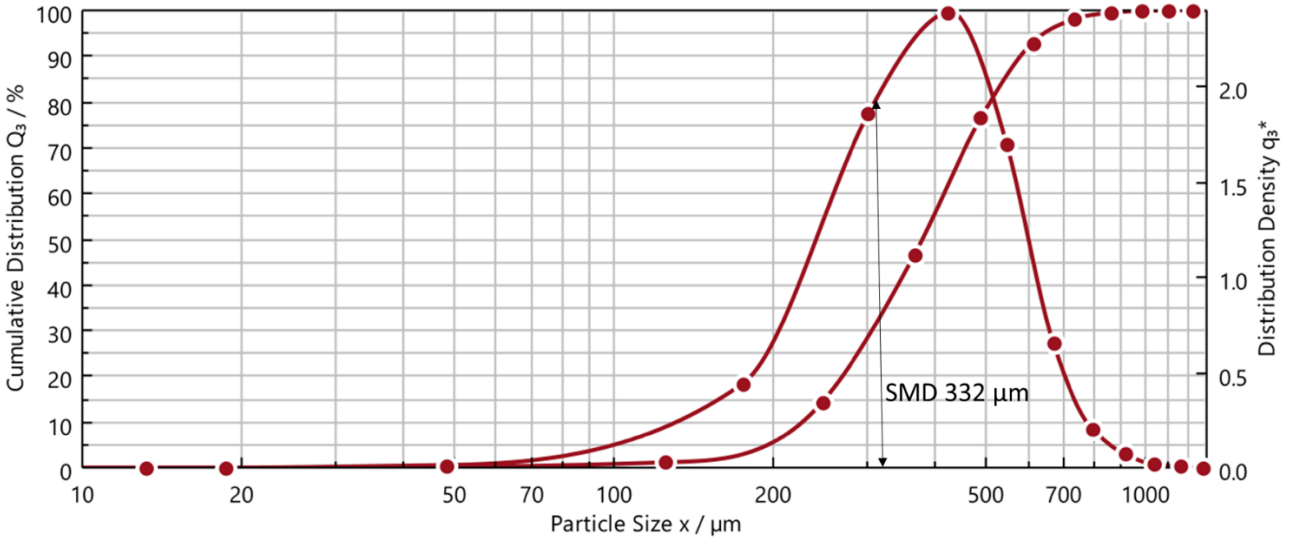

Figure 5: Particle size distribution of the biomass – size range 1 – termed "small".

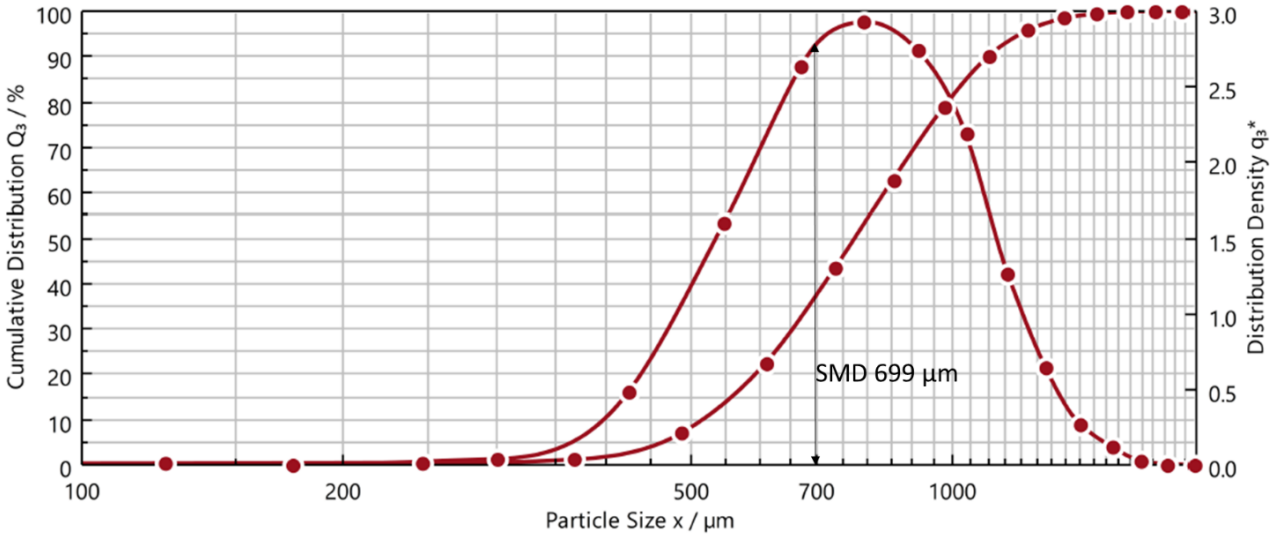

Figure 6: Particle size distribution of the biomass – size range 2 – termed "medium".

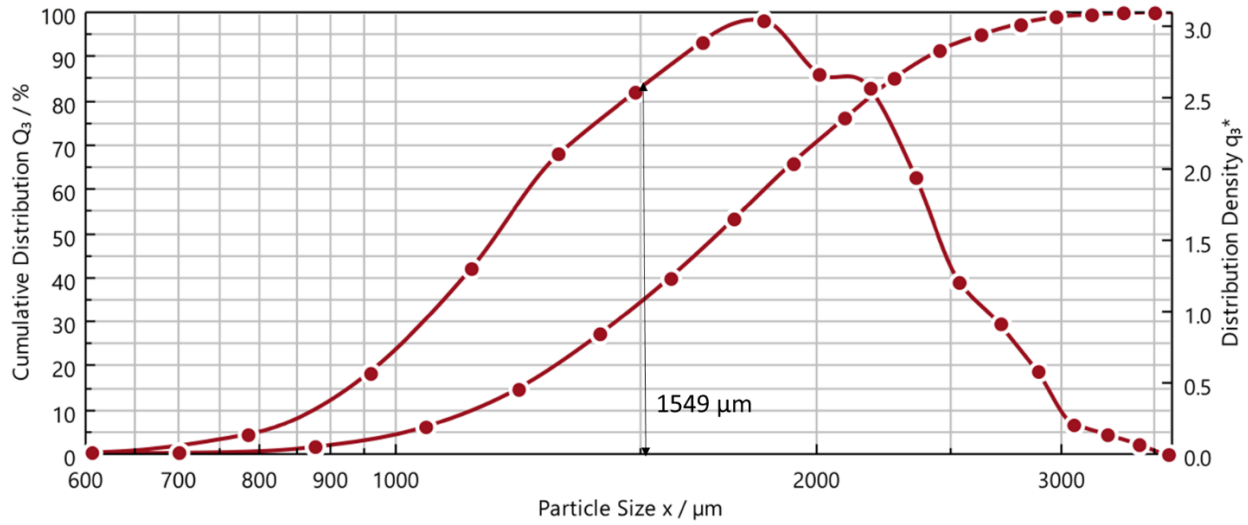

Figure 7: Particle size distribution of the biomass – size range 3 – termed "large".

2.3 EXPERIMENTAL PROCEDURE

The laboratory test matrix (Table 1) consisted of ten tests: a single glass beads fluidization test followed by nine tests corresponding to three mass loadings of biomass for the three different size ranges. One repeat test was performed at each setting.

Table 1: Test Matrix

#	Glass Beads SMD (µm)	Mass of Glass Beads (g)	Biomass SMD (µm)	Mass of Biomass (g)	Approximate Particle Count (Glass Beads + Biomass)*
1	353	73	-	-	
2			332	2	1275994 + 141821
3				4	1275994 + 283642
4				6	1275994 + 425462
5			699	2	1275994 + 15196
6				4	1275994 + 30392
7				6	1275994 + 45588
8			1549	2	1275994 + 1397
9				4	1275994 + 2793
10				6	1275994 + 4190

*Based on SMD

The inlet gas flow rate (velocity) was varied in a staircase mode, as shown in Figure 8. The tests were started with an inlet air velocity representing 1 U_{mf} (minimum fluidization velocity of glass beads). The inlet air velocity was increased step-wise at 1 U_{mf} intervals and held constant for five minutes at each step. The maximum velocity was 4 U_{mf} or 5 U_{mf}, depending on the size distribution and mass loading of biomass samples. For example, some entrainment was observed with the smaller size of biomass particles, therefore the maximum gas velocities were limited to 4 U_{mf}. The gas velocity was then reduced step-wise back to 1 U_{mf}.

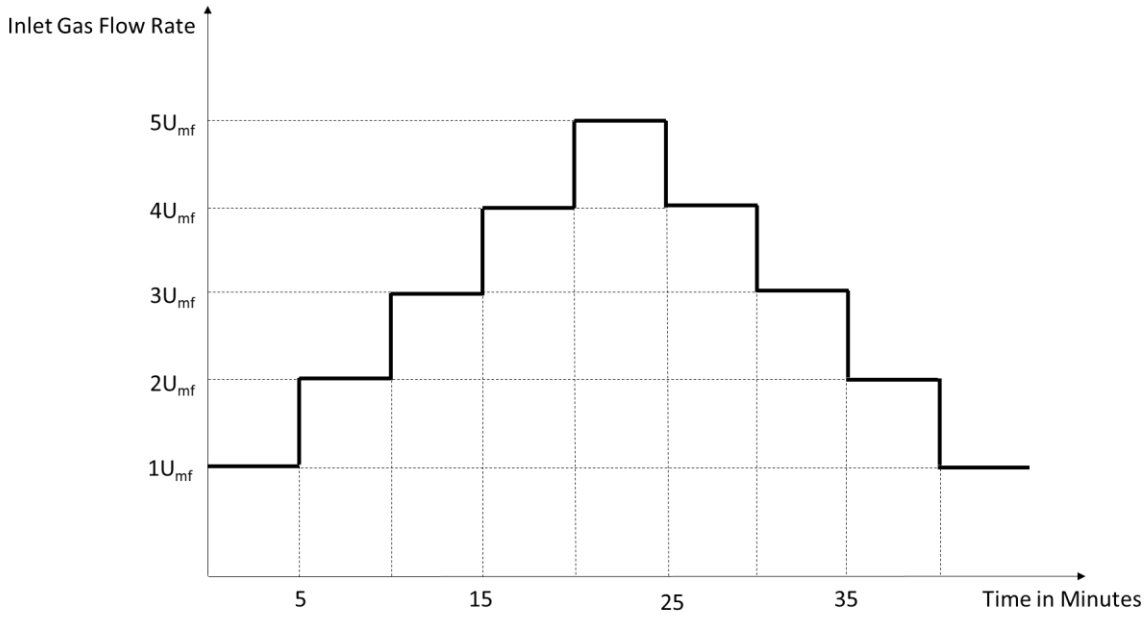

Figure 8: Variation of the inlet gas flow rate (velocity) during the laboratory fluidization tests.

The first test was performed using 73 g of glass beads without biomass particles. This mass of glass beads was chosen so that there was adequate bed material to record the pressure drop measurements ΔP_0–ΔP_5, thereby providing adequate validation points. With too little bed material, there would be a lower number of pressure measurement data points. On the other hand, too much bed material may result in particle entrainment. With this set-up, there was minimal loss (< 3 g) of glass beads in the pressure taps, the weight of glass beads at the end of the experiments was 70 g in most of the test runs.

The subsequent tests were performed using mixtures of biomass particles and glass. Each loading was repeated to ensure consistency in measurements. For each of the size ranges, three mass loadings were chosen for study. The mass of biomass was 2 g, 4 g, and 6 g, which corresponded to mass fractions of 2.7 wt% biomass, 5.2 wt% biomass, and 7.6 wt% biomass respectively as provided in Table 1. Particle count estimates were obtained using particle densities of 2,484 kg/m^3 and 736 kg/m^3 for the glass beads and biomass particles respectively.

It was observed that running the fluidization tests over a period of time caused some loss of the bed material to the walls of the test rig, as a result of static charge. These losses could be more critical in the biomass—glass beads mixtures as there are fewer biomass particles in the

mixtures. Therefore, a bubbler was used with the gas inlet to introduce some humidity into the test rig. Sensitivity cases were run with glass beads as well as glass bead—biomass mixtures to ensure that the pressure readings as well as the fluidization behaviors were not impacted.

3. EXPERIMENTAL RESULTS

Overall, the mixing of biomass and glass beads was good at lower mass loadings of biomass and at higher inlet gas velocities (4 U_{mf} and 5 U_{mf}). During the experiments, there was noticeable slugging.

- There was greater slugging observed with larger sizes of biomass. This can be observed by comparing the slugging behavior from Figure 9 and Figure 10 for large biomass and from Figure 12 and Figure 13 for the medium biomass. For large-sized biomass particles, slugging was prominent at gas velocities of up to 3 $U_{mf,}$, while the medium-sized biomass mixture was found to slug only up to gas velocities of 2 U_{mf}.
- There was greater slugging observed at higher mass loadings, this effect is shown in Figure 10 and Figure 11. It was observed that for the mixture with higher mass of biomass (4 g), slugging was prominent at gas velocities of up to 3 U_{mf} while at a lower mass loading (2 g), the particles were well-mixed at 3 U_{mf}.

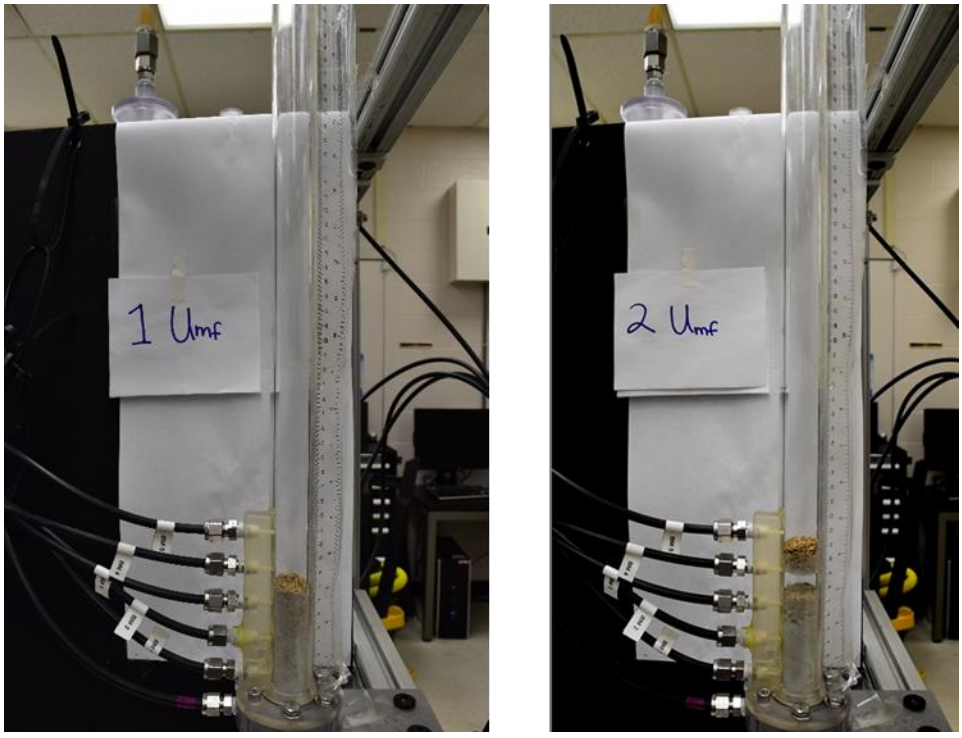

(a) (b)

Figure 9: Snapshots from experiment – mixture of glass beads and 4 g of large-sized biomass: (a) 1 U_{mf}, and (b) 2 U_{mf}.

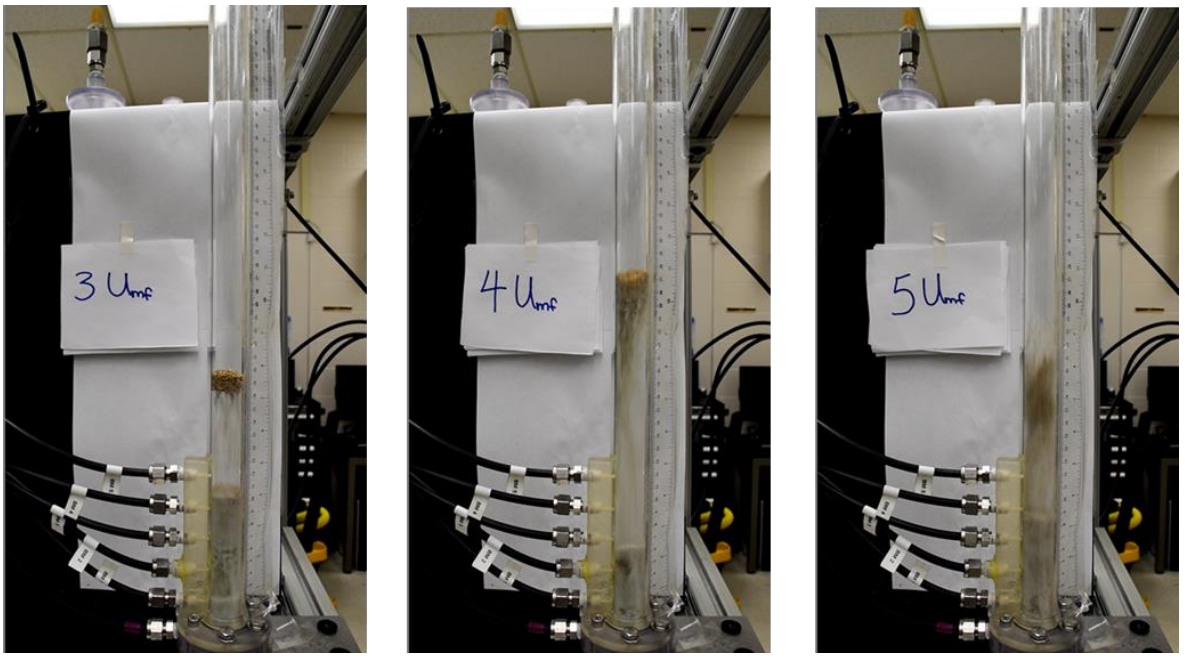

(a) (b) (c)

Figure 10: Snapshots from the experiment – 4 g of large size biomass: (a) 3 U_{mf}, (b) 4 U_{mf}, and (c) 5 U_{mf}.

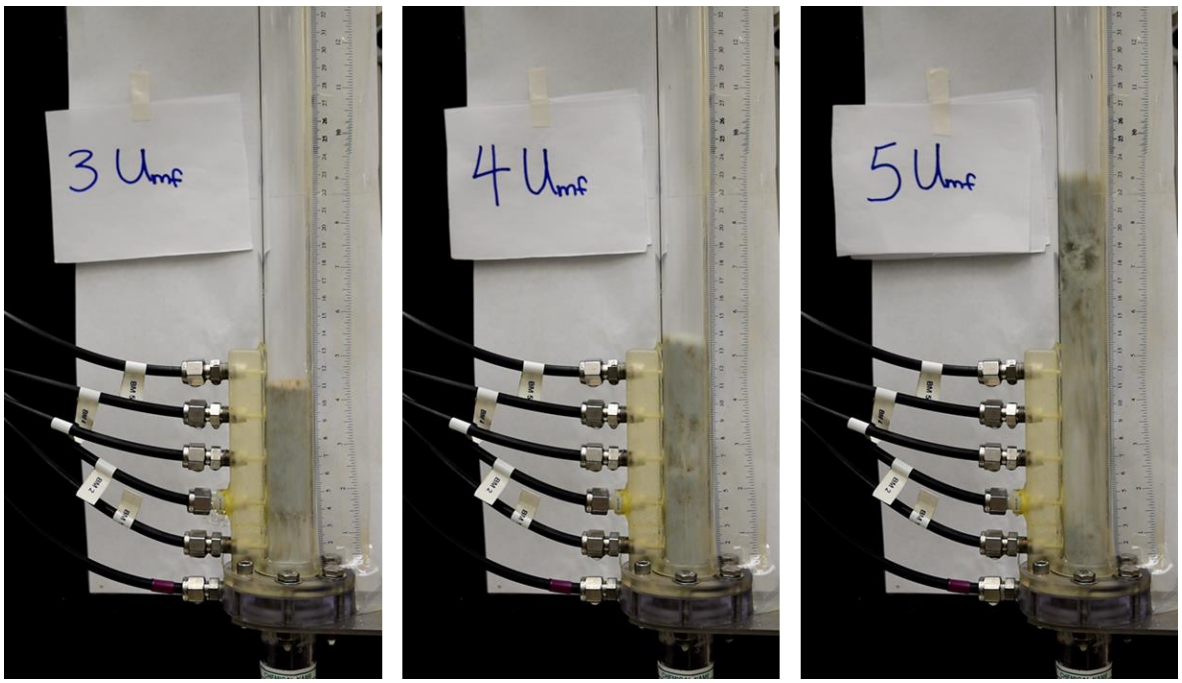

(a) (b) (c)

Figure 11: Snapshots from the experiment – 2 g of large size biomass: (a) 3 U_{mf}, (b) 4 U_{mf}, and (c) 5 U_{mf}.

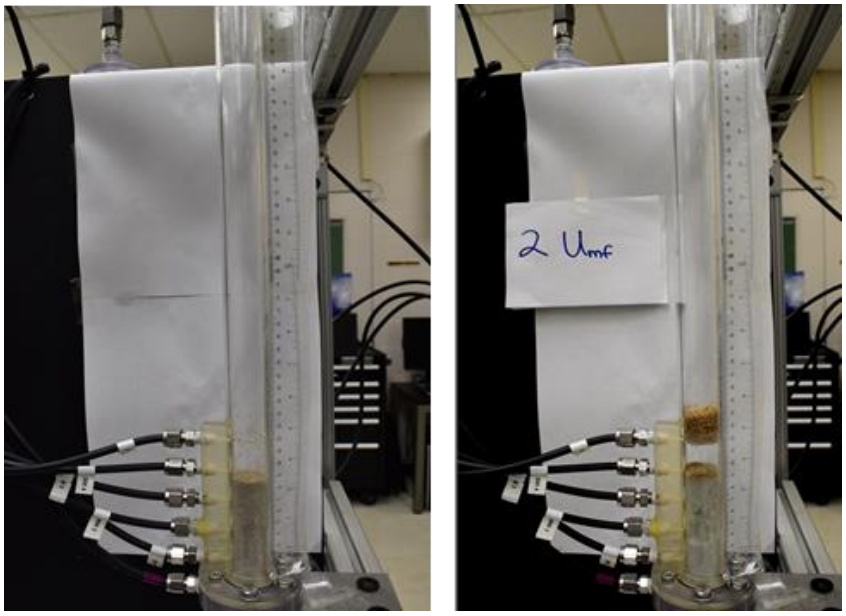

(a) (b)

Figure 12: Snapshots from the experiment – 4 g of medium size biomass: (a) 1 U_{mf}, and (b) 2 U_{mf}.

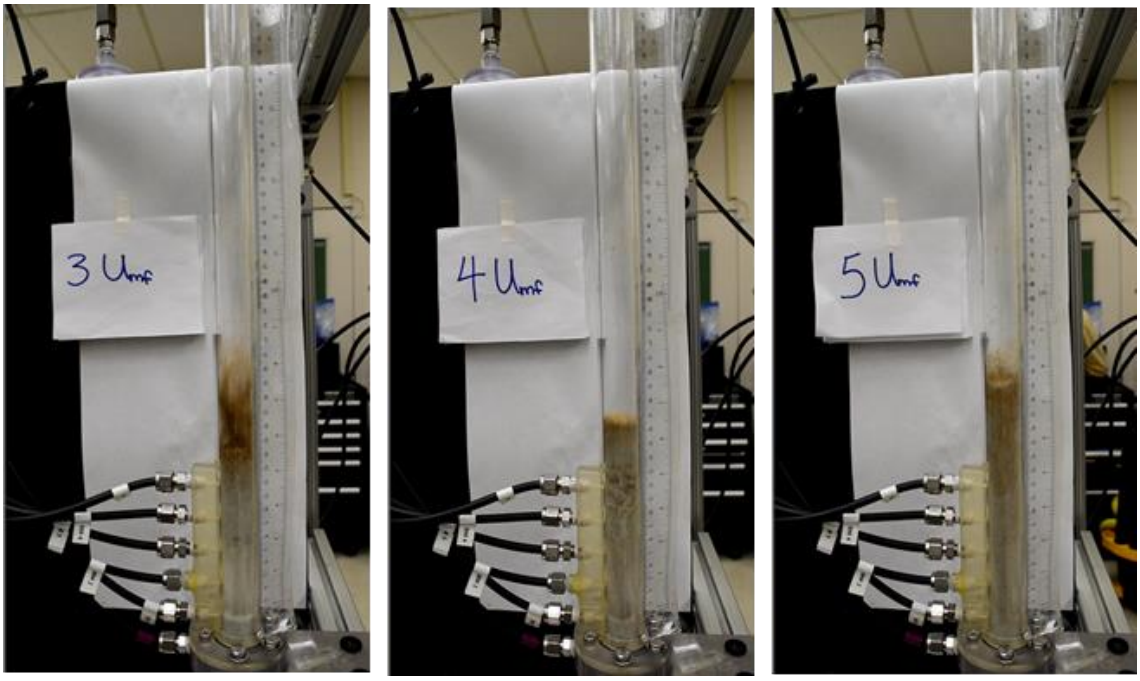

(a) (b) (c)

Figure 13: Snapshots from the experiment – 4 g of medium size biomass: (a) 3 U_{mf}, (b) 4 U_{mf}, and (c) 5 U_{mf}.

The effect of slugging was also observed in the pressure data. Figure 14 shows the pressure drop values along the bed as indicated in Figure 1 for the smallest size of biomass at different gas velocities. Slugging in the flow was observed mostly in the region corresponding to ΔP5, where the pressure drop differences between the different mass loading rates were the most significant. Similar patterns for pressure drop were observed with the medium- and large-sized biomass samples. The results for the medium and large size biomass are presented in the Appendix.

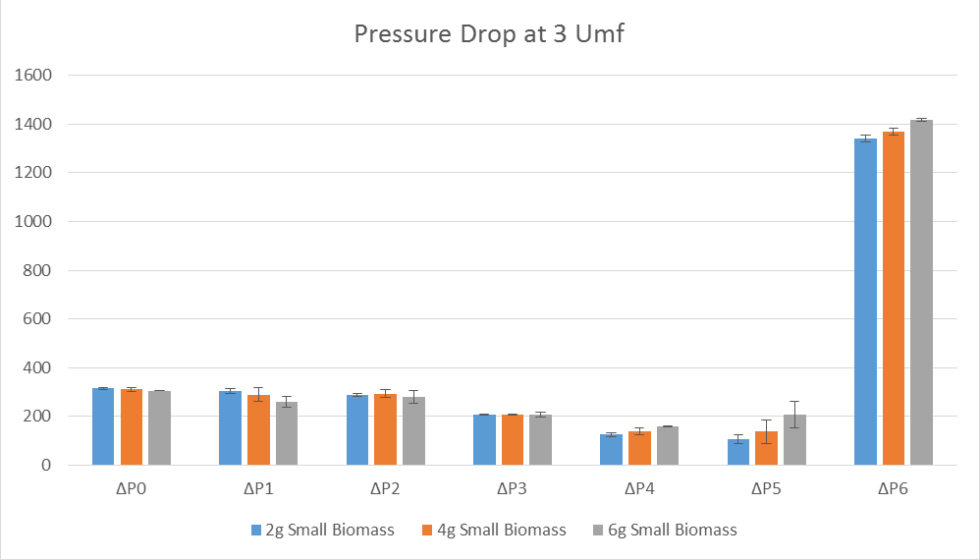

Figure 14: Pressure drop (Pa) for different mass loadings of the small size biomass at a gas velocity of 3 U_{mf}.

4. SIMULATION SET-UP AND RESULTS

4.1 THE HYBRID DRAG MODEL

The glass beads—biomass mixtures were modeled using the NETL Multiphase Flow with Interphase eXchanges (MFiX) solver. All simulations were performed using an Eulerian approach for the continuum phase, i.e., the gas phase and a Lagrangian approach for the particle, i.e, solid phase. The experimental pressure drop from the different segments along the height of the fluidized bed was compared with the predicted values from the simulations. Qualitative comparisons such as solids distribution and voidage, mixing and segregation behavior, and the bed height from the simulations were compared with the video recordings taken during the experimental runs.

Both the solid phases were modeled as spherical particles. A hybrid drag model was used to account for the gas–solid momentum transfer. The Syamlal-O'Brien (1988) drag model was chosen for the almost spherical glass beads and the Ganser (1993) drag model was chosen to account for a shape factor of the irregularly shaped biomass particles. The drag equations are shown in the section below. All simulations were carried out using variable time steps as calculated by MFiX.

Syamlal-O'Brien Drag Law for the Glass Beads

The Syamlal-O'Brien drag model includes two system dependent parameters (C_1 and C_2) to ensure the calculated minimum fluidization velocity (U_{mf}) matches the experimental measured value. The parameters C1 and C2 can be calculated using the spreadsheet downloadable at https://mfix.netl.doe.gov/doc/mfix-archive/umf_spreadsheets/umf.xls.

$$\beta_{Syamlal-O'Brien} = \frac{3}{4}\frac{C_{so}\varepsilon_f(1-\varepsilon_f)\rho_f}{d_p}\left|\mathbf{v}_f - \mathbf{v}_p\right|$$

$$C_{so} = \left(\frac{0.63}{v_r} + \frac{4.8}{\sqrt{v_r\,\mathrm{Re}_p}}\right)^2$$

$$v_r = 0.5\left(A - 0.06\,\mathrm{Re}_p + \sqrt{(0.06\,\mathrm{Re}_p)^2 + 0.12\,\mathrm{Re}_p(2B - A) + A^2}\right)$$

$$A = \varepsilon_f^{4.14}$$

$$B = \begin{cases} C_2\varepsilon_f^{1.28}, & \varepsilon_f \le 0.85 \\ \varepsilon_f^{C_1}, & \varepsilon_f > 0.85 \end{cases}$$

$$\mathrm{Re}_p = \frac{\left|\mathrm{v}_f - \mathrm{v}_p\right|\rho_f d_p}{\mu_f}$$

where,

ε_f is the gas phase void fraction

v_f is the gas phase velocity

v_p is the solid phase velocity

ρ_f is the gas phase velocity

d_p is the SMD

μ_f is the gas phase viscosity

Ganser Drag Law

The Ganser drag model is a correction considering the non-spherical particle shapes. In this research, this correction is coupled with the Gidaspow model. The coefficient is calculated as:

$$\beta_{\text{Ganser}} = \begin{cases} 150\dfrac{(1-\varepsilon_f)^2\mu_f}{\varepsilon_f d_p{}^2\phi^2} + 1.75\dfrac{(1-\varepsilon_f)\rho_f\left|\mathbf{v}_f-\mathbf{v}_p\right|}{d_p\phi}, & \varepsilon_f \le 0.8 \\ \dfrac{3}{4}\dfrac{\varepsilon_f(1-\varepsilon_f)\rho_f\left|\mathbf{v}_f-\mathbf{v}_p\right|}{d_p\phi}C_{D0}\varepsilon_f{}^{-2.65}, & \varepsilon_f > 0.8 \end{cases} \quad (1)$$

$$K_1 = \left(\tfrac{1}{3}+\tfrac{2}{3}\phi^{-0.5}\right)^{-1} - 2.25\frac{d_p}{D_{reactor}}$$
$$K_2 = 10^{1.8148(-\log\phi)^{0.5743}} \quad (2)$$

$$C_D = \frac{24}{\text{Re}\,K_1}\left(1+0.1118(\text{Re}\,K_1K_2)^{0.6567}\right) + \frac{0.4305K_2}{1+3305/(\text{Re}\,K_1K_2)} \quad (3)$$

$$\text{Re}_p = \frac{\left|v_f - v_p\right|\rho_f d_p \varepsilon_f}{\frac{\mu_f}{\phi}}$$

where,

ε_f is the gas phase void fraction

v_f is the gas phase velocity

v_p is the solid phase velocity

ρ_f is the gas phase velocity

d_p is the SMD

μ_f is the gas phase viscosity

ø is the sphericity of the biomass particle (calculated from QICPIC)

D_{reactor} is the diameter of the fluidized bed.

4.2 RESULTS

4.2.1 Pressure Drop Comparison

The data from simulations were obtained well past the initial transients using MFiX DEM. Differential pressure measurements along the riser (ΔP0–ΔP6 from Figure 1) from experiments

were compared with the simulation results in Figure 15 through Figure 22 for different sizes and mass loadings. The total pressure drop (ΔP6) is representative of total mass in the riser. Pressure drop across individual pressure ports (ΔP0–ΔP5) is representative of mass distribution along the riser. The error bars from the experimental data represent the standard error due to uncertainty in measurements.

It was observed that the simulations were able to capture the different trends in the differential pressure measurements. The total pressure drop was predicted reasonably well. There were noticeable errors in the magnitude of pressure drop predictions, which were more prominent for mixtures which slugged or mixed poorly. These occurred at lower gas velocities and at higher mass loadings. The error in prediction for ΔP5 was always the highest for any given dataset. It should be noted that the magnitude of pressure drop ΔP5 was relatively lower (less material) and the experimental uncertainty was also higher in the corresponding region, indicating it may be more challenging to predict the amount of bed material in that region.

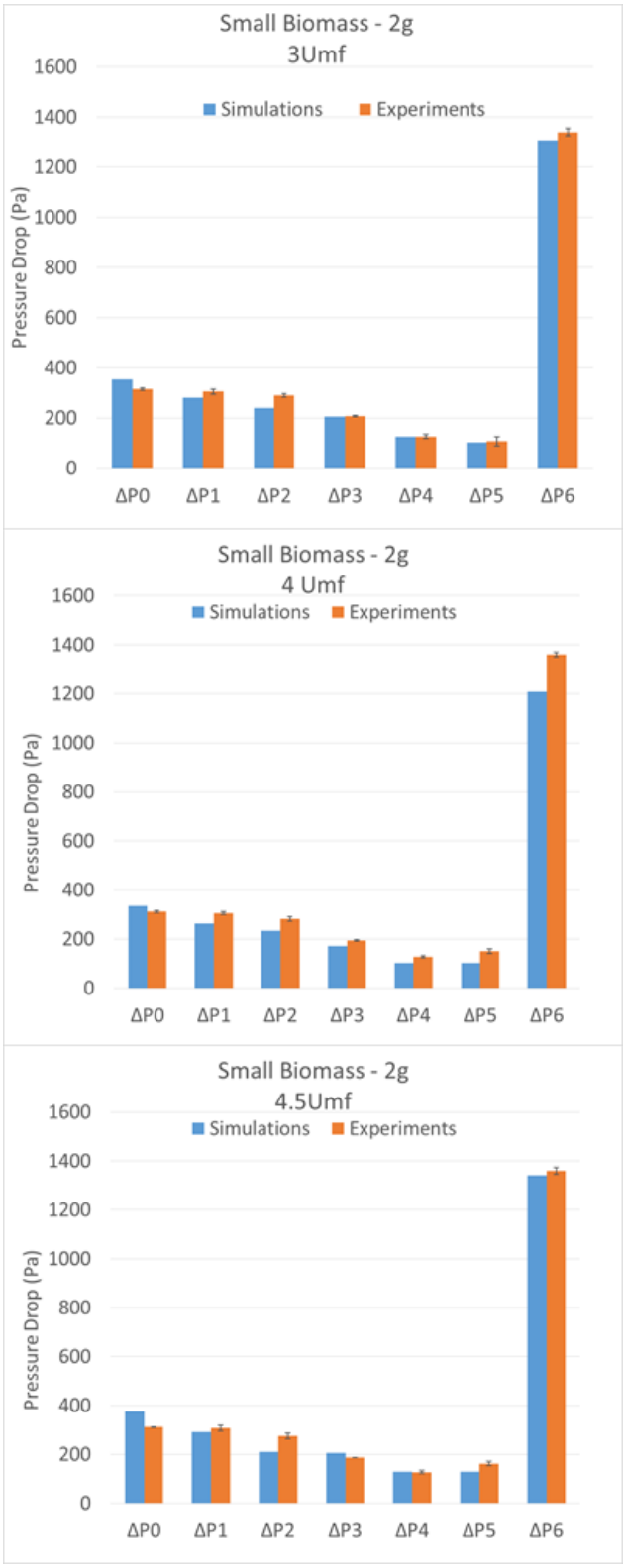

Figure 15: Comparison of the pressure drops for the small size biomass (2 g) – experiments vs. DEM simulations.

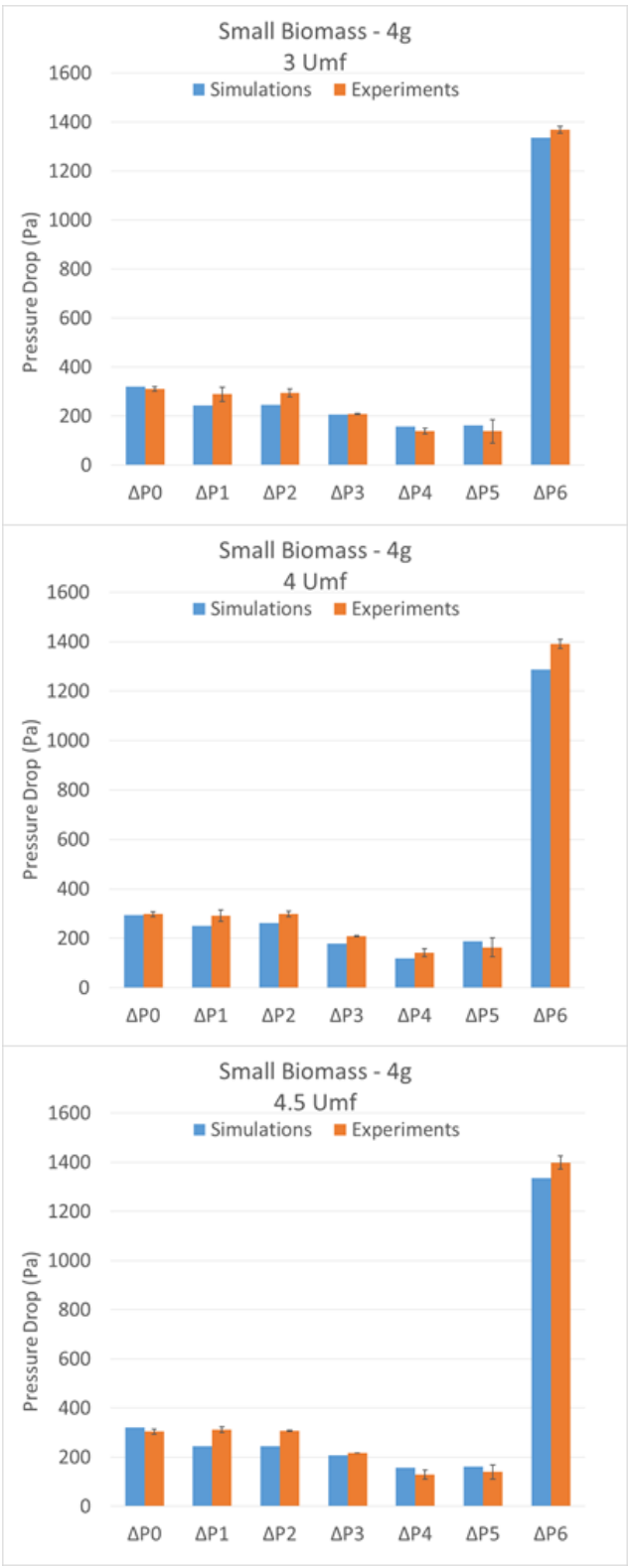

Figure 16: Comparison of the pressure drops for the small size biomass (4 g) – experiments vs. DEM simulations.

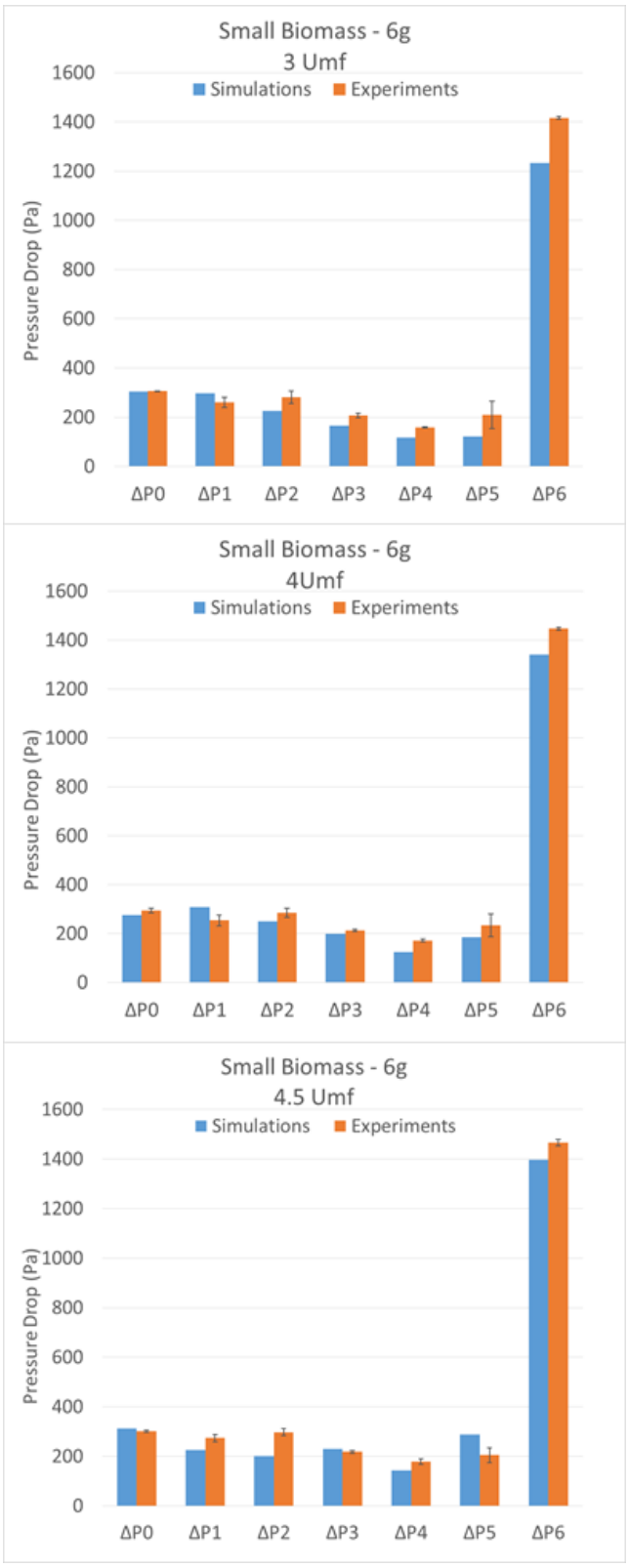

Figure 17: Comparison of the pressure drops for the small size biomass (6 g) – experiments vs. DEM simulations.

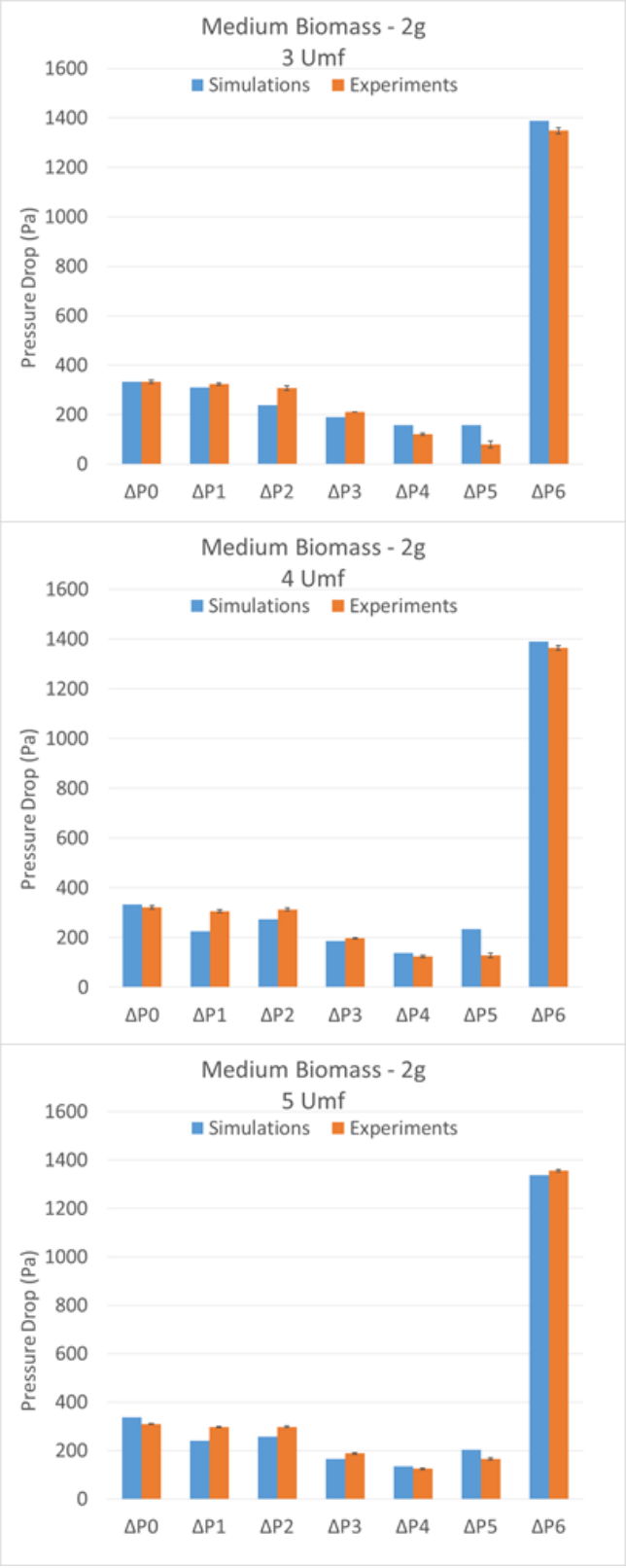

Figure 18: Comparison of the pressure drops for the medium size biomass (2 g) – experiments vs. DEM simulations.

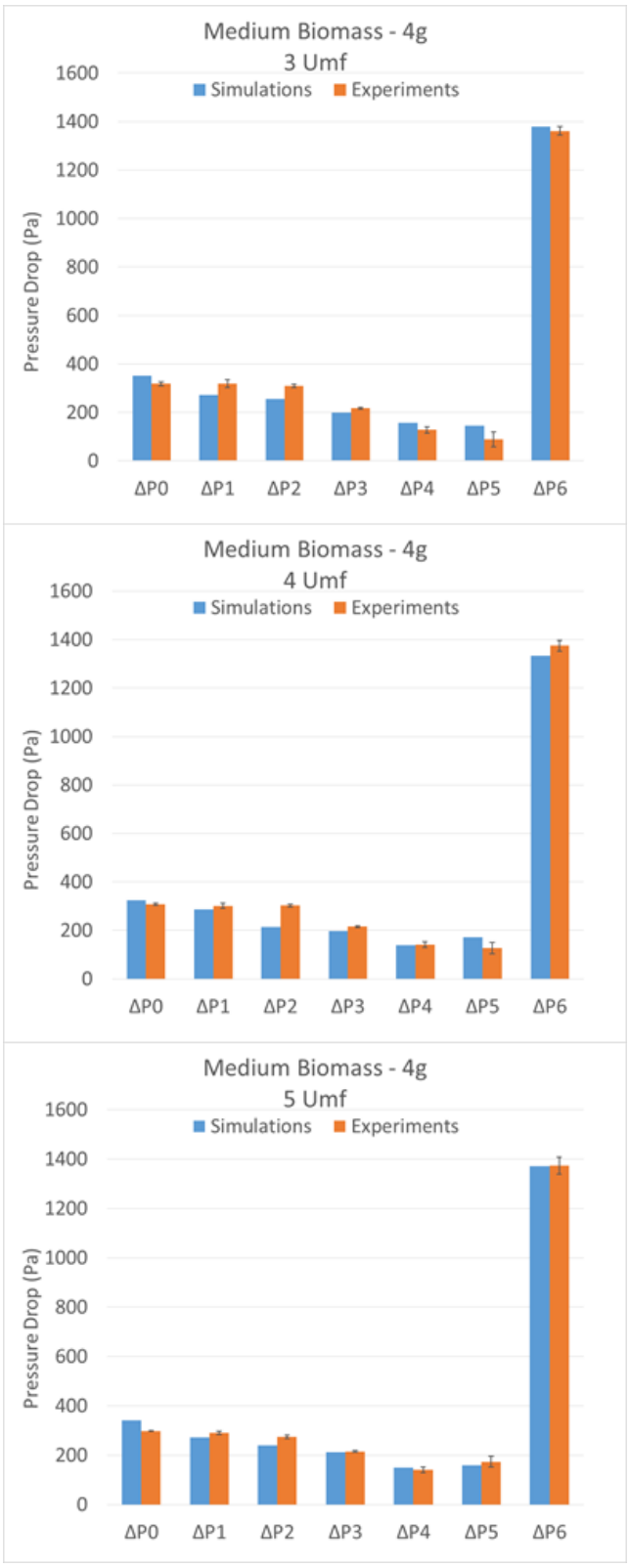

Figure 19: Comparison of the pressure drops for the medium size biomass (4 g) – experiments vs. DEM simulations.

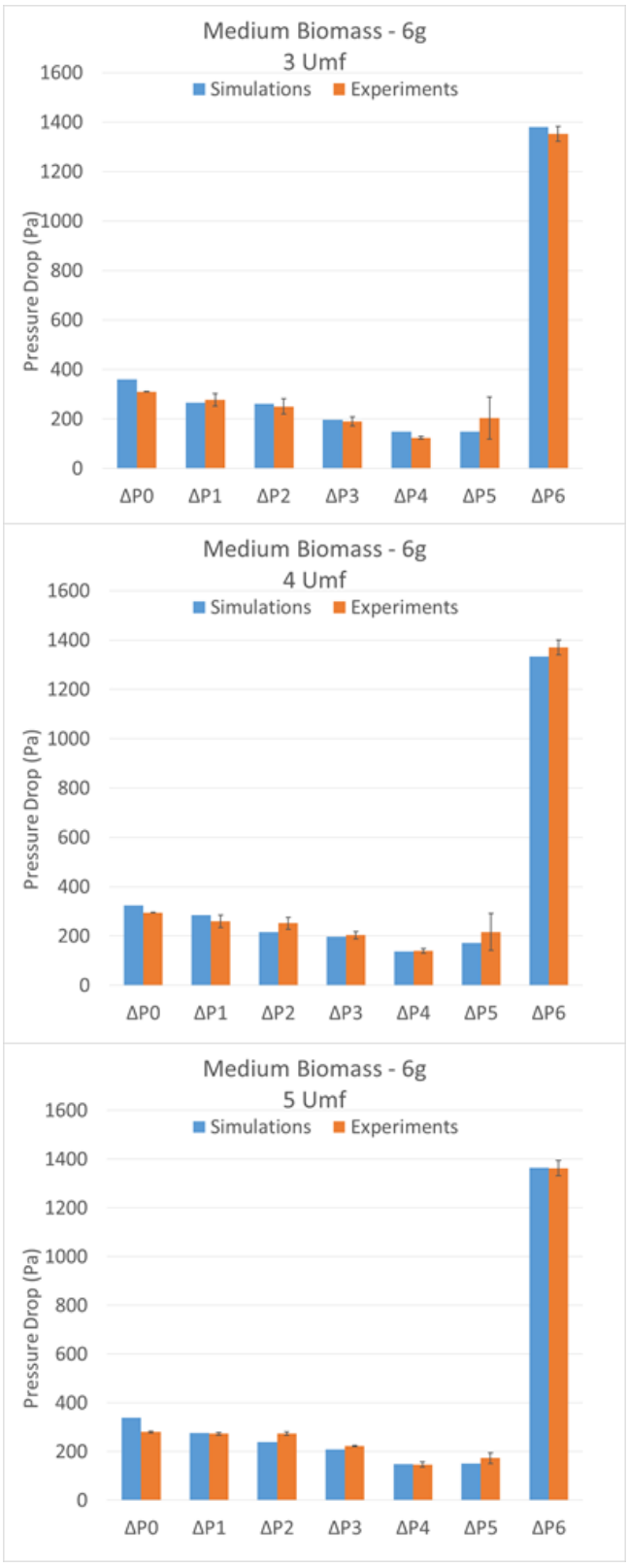

Figure 20: Comparison of the pressure drops for the medium size biomass (6 g) – experiments vs. DEM simulations.

Figure 21: Comparison of the pressure drops for the large size biomass (2 g) – experiments vs. DEM simulations.

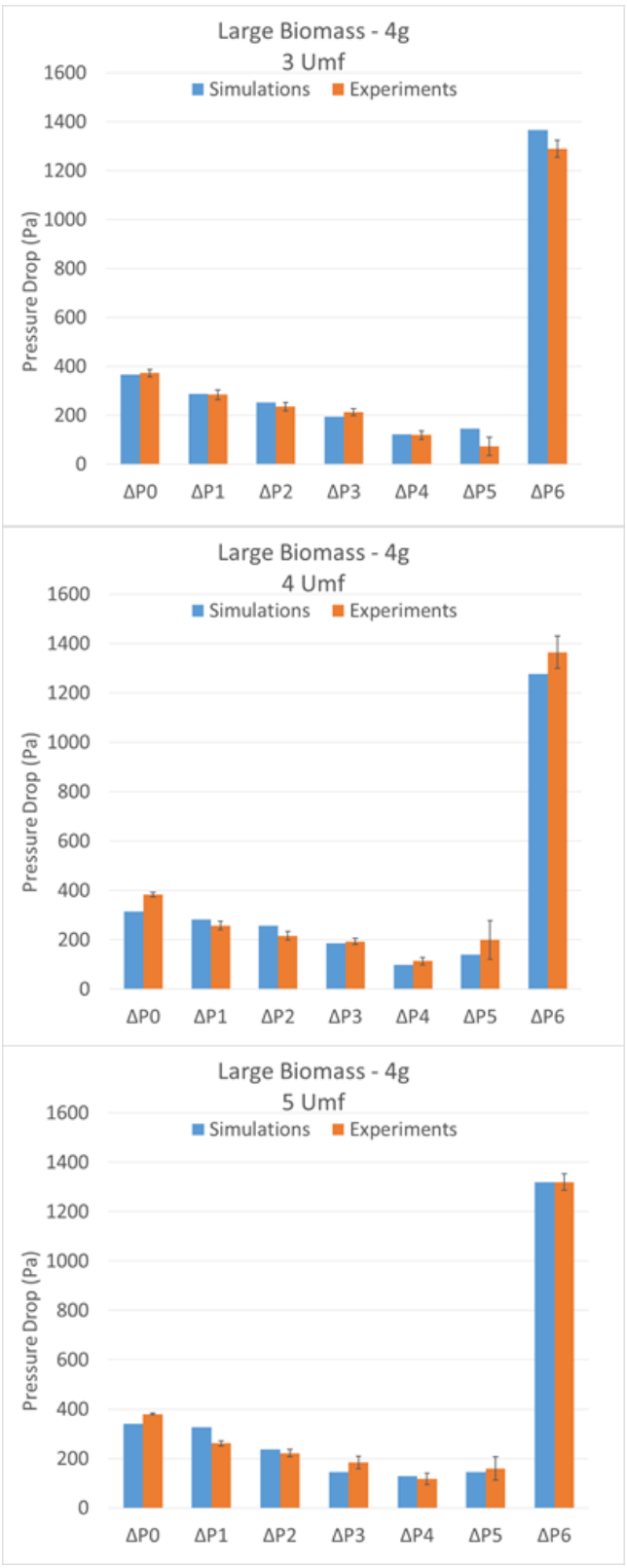

Figure 22: Comparison of the pressure drops for the large size biomass (4 g) – experiments vs. DEM simulations.

4.2.2 Qualitative Comparisons

In this section, snapshots from the experiments and the simulations are compared for quantities of interest such as bed height and voidage (solids concentration). One sample is shown for each size distribution of biomass used.

It was observed that the bed voidage and height are predicted reasonably well in the simulations. The degree of mixing as in the case of the large biomass mixture shown in Figure 23 was well predicted in the simulations. The glass beads are represented by blue particles and the biomass phase is represented by red particles. Similarly, the segregation of biomass from glass beads as seen for the medium and smaller biomass sizes as shown in Figure 24 and Figure 25 respectively, was also observed in the simulations. For the small size, there was some elutriation of the biomass phase to the exit of the riser in the experiments. This was also observed in the simulation, as shown in Figure 25 as the floating red particles over the blue glass beads.

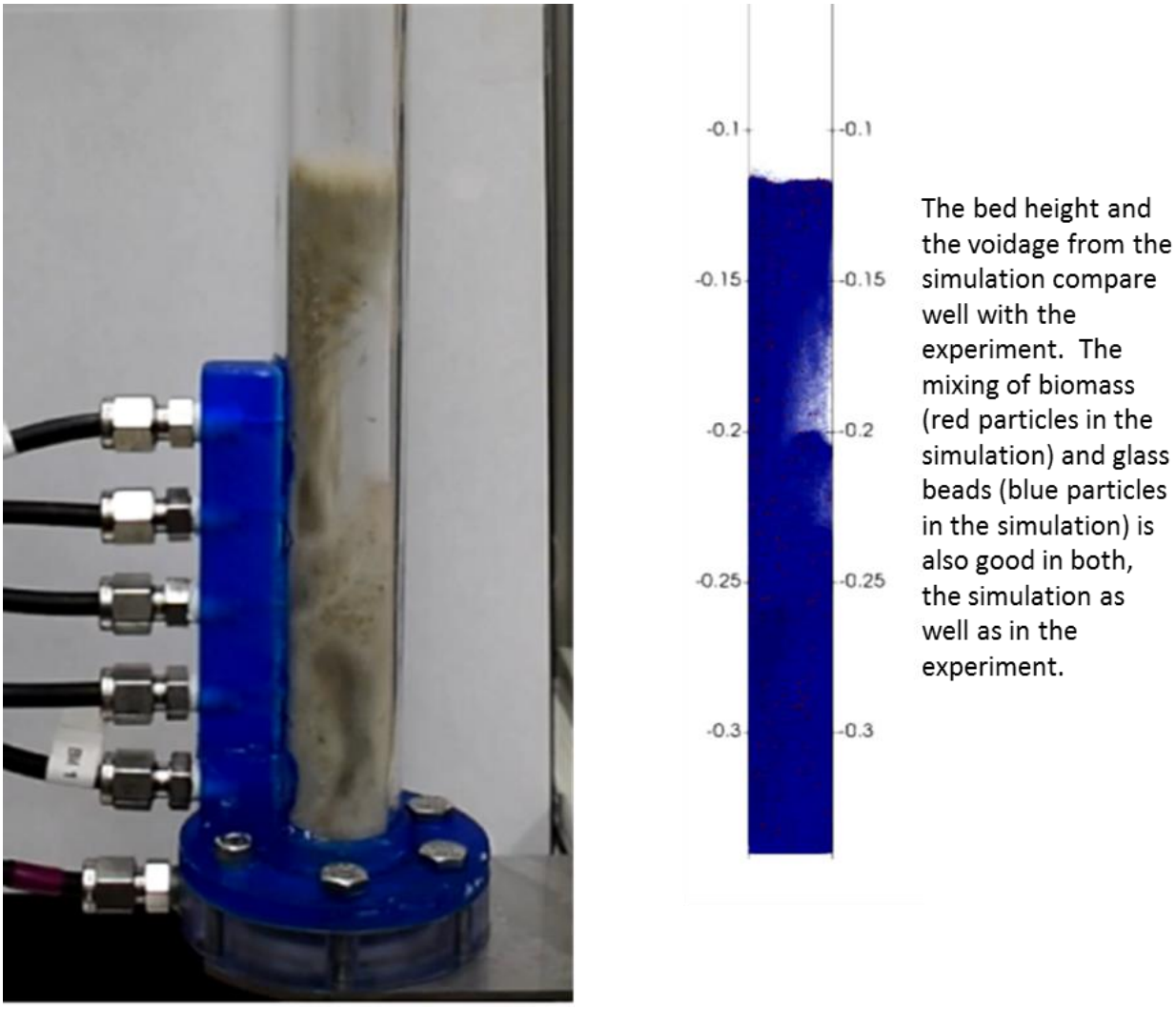

Figure 23: Comparison of a snapshot from the experiment (left) and the simulation (right) for the large biomass mixture (4 g) at 5 U_{mf}.

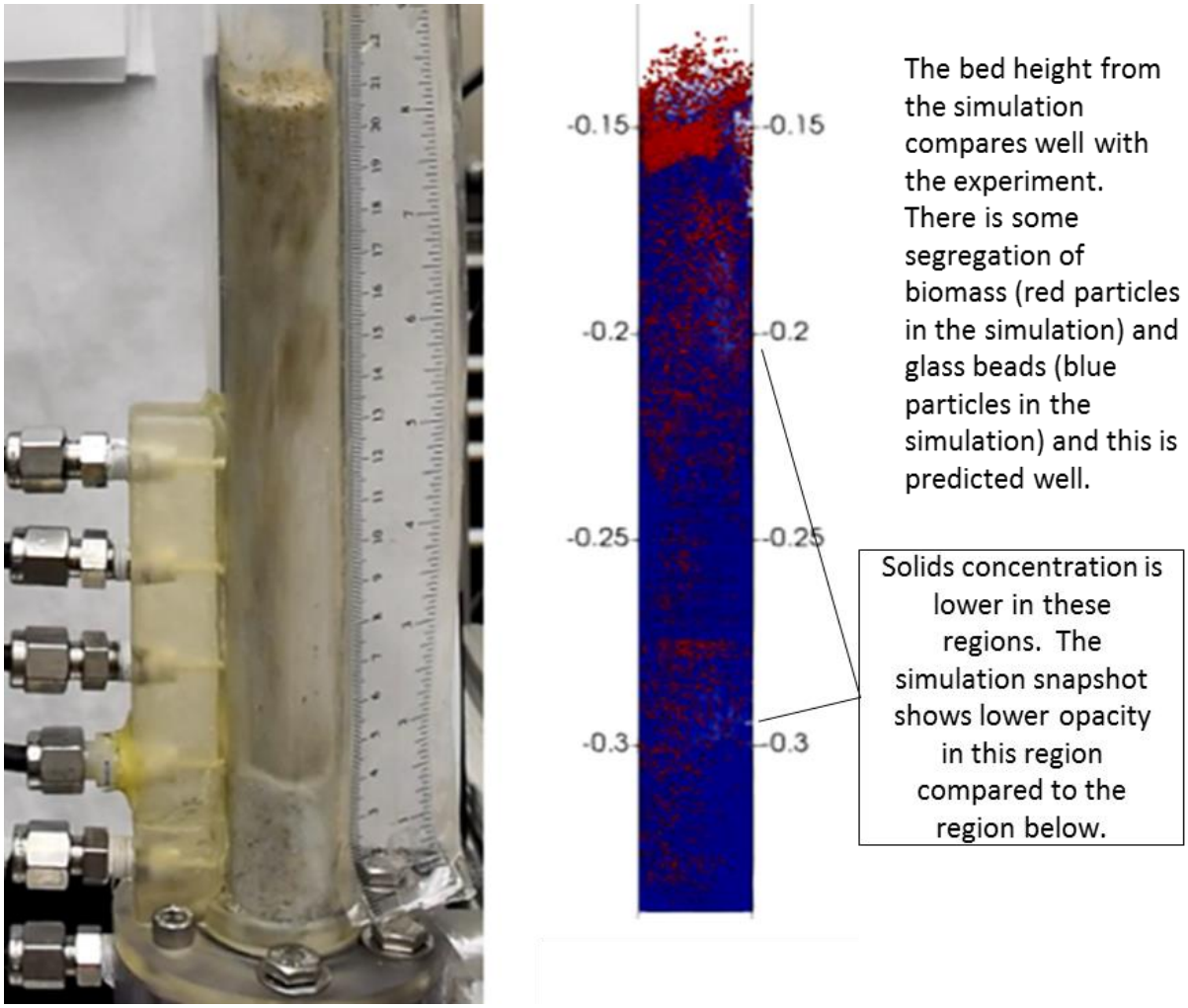

Figure 24: Comparison of a snapshot from the experiment (left) and the simulation (right) for the medium biomass mixture.

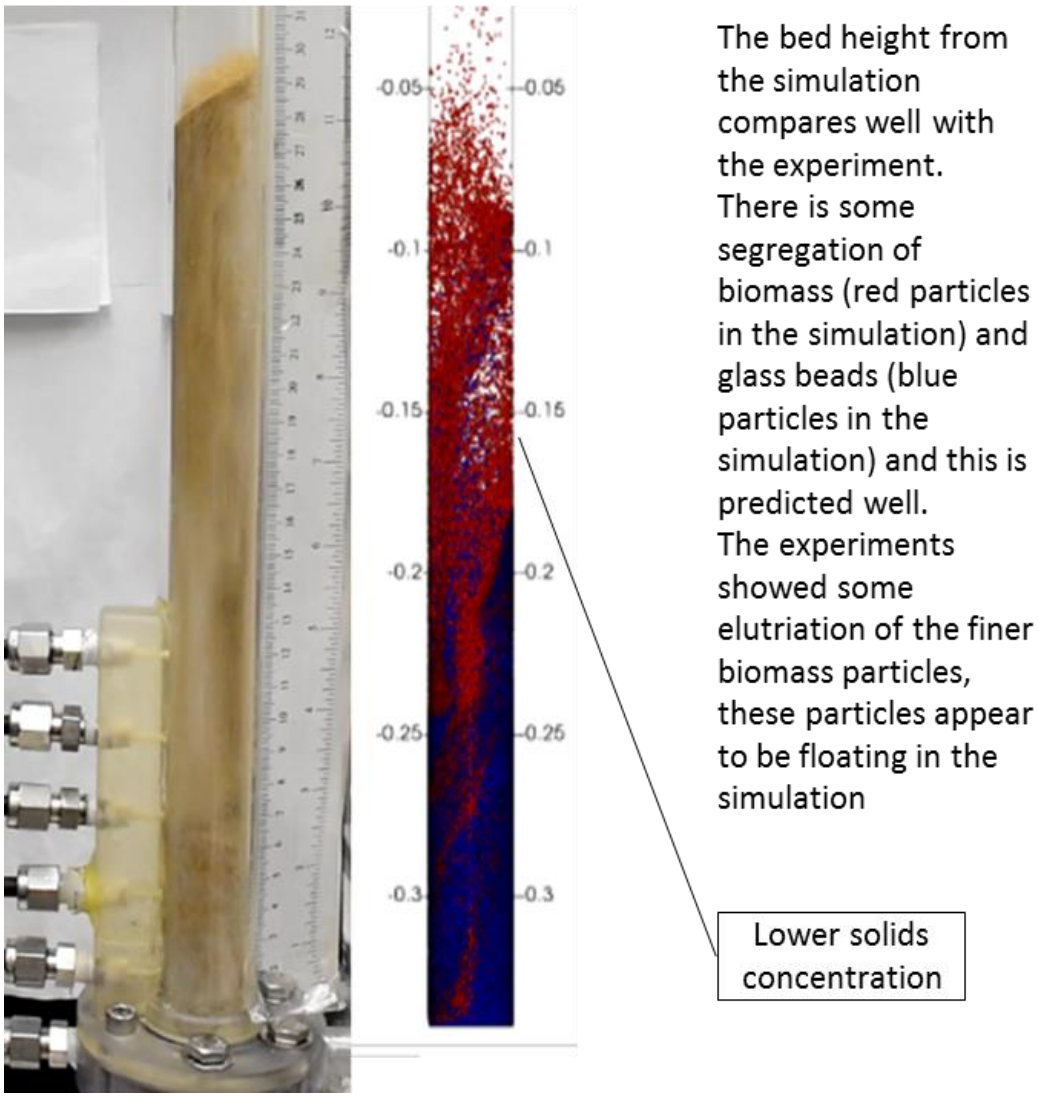

Figure 25: Comparison of a snapshot from the experiment (left) and the simulation (right) for the small biomass mixture.

5. CONCLUSIONS AND FUTURE WORK

A literature survey was conducted to identify typical biomass and inert bed material characteristics in fluidized bed applications with biomass. This information was used to design lab-scale experiments to collect hydrodynamic data pertaining to biomass—inert bed material mixtures. The biomass used comprised of crushed wood pellets sieved to obtain three size ranges —small (SMD 332 µm), medium (SMD 699 µm) and large (SMD 1,549 µm). The inert bed material chosen was glass beads (SMD 353 µm). The lab tests were performed by fluidizing eight mixtures of their biomass-inert material (3 mass loadings, * 3 biomass sizes excluding one 6 g large biomass mixture) with gas velocities of 1 U_{mf}–5 U_{mf}. Overall, the mixing of biomass and glass beads was good for lower biomass mass fraction and higher inlet gas velocities (4 U_{mf} and 5 U_{mf}). Tendency to slug was more pronounced at higher mass loadings and with larger sizes of biomass.

The biomass-glass beads mixtures were then modeled using the MFiX-DEM code. The solid-gas momentum exchange was modeled using a hybrid drag model. The Ganser drag model was used for the biomass phase and the Syamlal drag model was used for the glass beads. The hybrid drag model with standard model parameters was able to predict the trends in pressure drop along the riser well. The match to experimental pressure drop is reasonable overall. The error in prediction was higher at lower fluidization velocities and at higher mass loadings, where the mixing is poorer and slugging is more frequent. There is a greater error in prediction in the region ΔP5 across all cases. The uncertainty from experimental results are also higher for this region and the magnitude of pressure drop in this region is lower. The bed height, voidage (solids concentration), and the mixing/segregation behavior are predicted reasonably well using the hybrid drag model.

To evaluate the versatility of the drag model, more challenging operating conditions could be designed. An example would be to perform lab-scale experiments using biomass of varied shapes and sizes sourced from different anatomical fractions. Biomass of varied shapes such as needles and barks are typical to commercial scale boilers where processing costs to minimize size/shape irregularities may be expensive and impractical.

The current study could also be extended to perform a multiscale modeling of biomass CFB combustor using MFiX. The drag model validated here will be coupled with kinetic schemes for biomass applications like combustion in order to perform reactor scale modeling.

6. REFERENCES

Adánez, J.; Gayán, P.; de Diego, L. F.; García-Labiano, F.; Abad, A. Combustion of Wood Chips in a CFBC. Modeling and Validation. *Industrial & Engineering Chemistry Research* **2003,** *42*, 987–999.

Belin, F.; James, D. E.; Walker, D. J.; Warrick, R. J. Waste wood combustion in circulating fluidized bed boilers. In *Circulating Fluidized Bed Technology*; Basu, P., Francois, J., Eds.; Pergamon: France, 1988; pp. 351–368.

Cui, H.; Grace, R. Fluidization of biomass particles: A review of experimental multiphase flow aspects. *Chemical Engineering Science* **2007,** *62*, 45–55.

Desroches-Ducarne, E.; Marty, E.; Martin, G.; Delfosse, L. Co-combustion of coal and municipal solid waste in a circulating fluidized bed. *Fuel* **1998,** *77*, 1311–1315.

Ganser, G. H. A rational approach to drag prediction of spherical and nonspherical particles. *Powder Technology* **1993,** *77*, 143–152.

Gungor, A.; Eskin, N. Hydrodynamic modeling of a circulating fluidized bed. *Powder Technology* **2007,** *172*, 1–13.

Gungor, A. Two-dimensional biomass combustion modeling of CFB. *Fuel* **2008,** *87*, 1453–1468.

Knöbig, T.; Werther, J.; Amand, L.-E.; Leckner, B. Comparison of large- and small-scale circulating fluidized bed combustors with respect to pollutant formation and reduction for different fuels. *Fuel* **1998,** *77*, 1635–1642.

Leckner, B.; Karlsson, M. Gaseous emissions from circulating fluidized bed combustion of wood. *Biomass and Bioenergy* **1993,** *4*, 379–389.

Lyngfelt, A.; Leckner, B. Combustion of wood-chips in circulating fluidized bed boilers — NO and CO emissions as functions of temperature and air-staging. *Fuel* **1999,** *78*, 1065–1072.

Syamlal, M.; O'Brien, T. J. Simulation of granular layer inversion in liquid fluidized beds. *International Journal of Multiphase Flow* **1988,** *14*, 473–481.

Youssef, M. A.; Wahid, S. S.; Mohamed, M. A.; Askalany, A. A. Experimental study on Egyptian biomass combustion in circulating fluidized bed. *Applied Energy* **2009,** *86*, 2644–2650.

APPENDIX

The pressure drop data from all of the test runs are presented in Figure A1–A7 below.

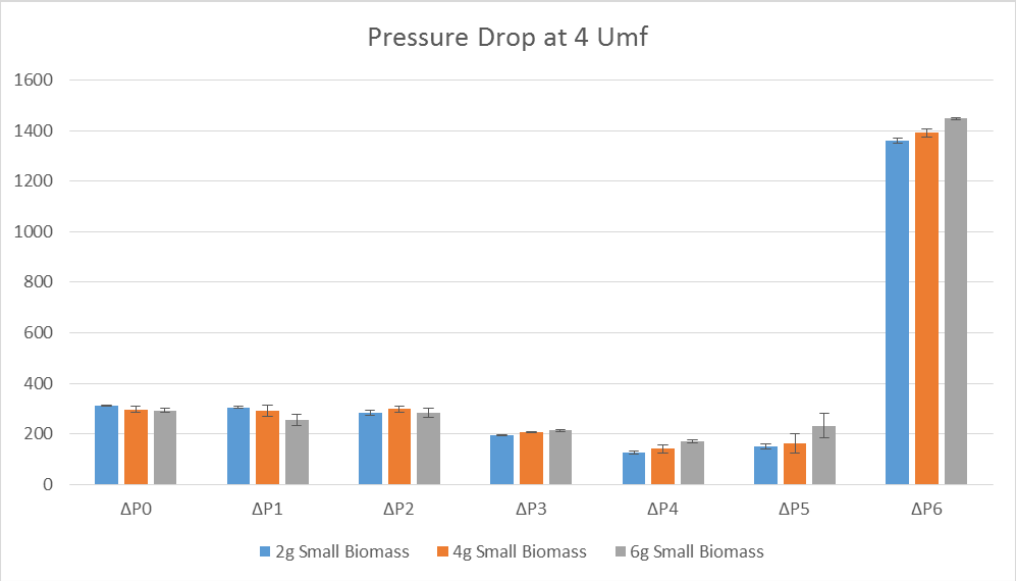

Figure A1: Pressure drop (Pa) for different mass loading of the small size biomass at a gas velocity of 4 U_{mf}.

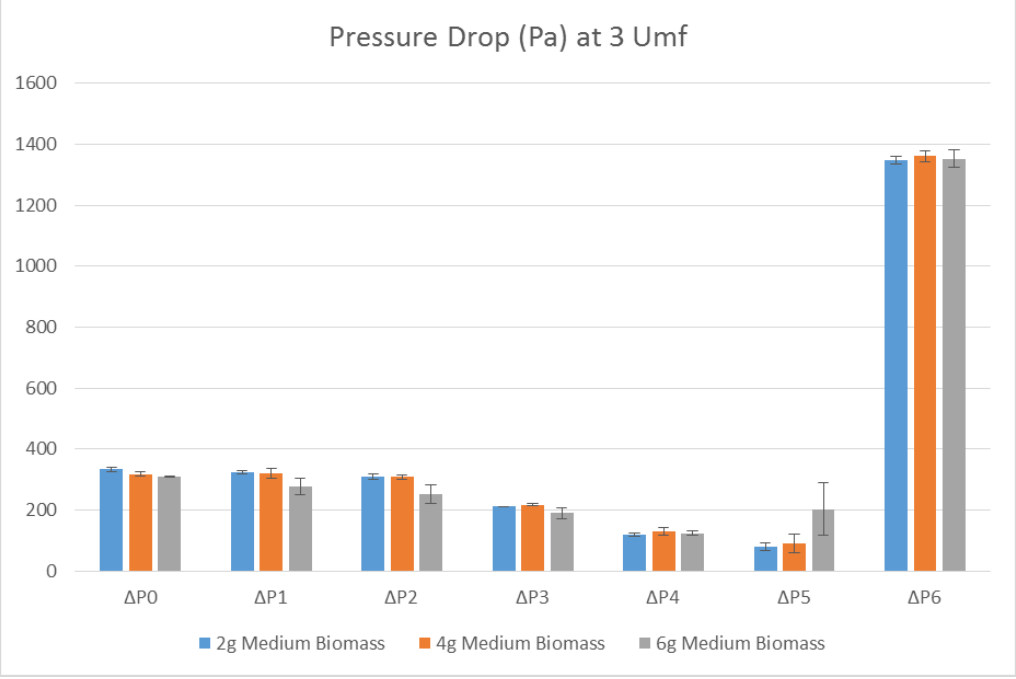

Figure A2: Pressure drop (Pa) for different mass loading of the medium size biomass at a gas velocity of 3 U_{mf}.

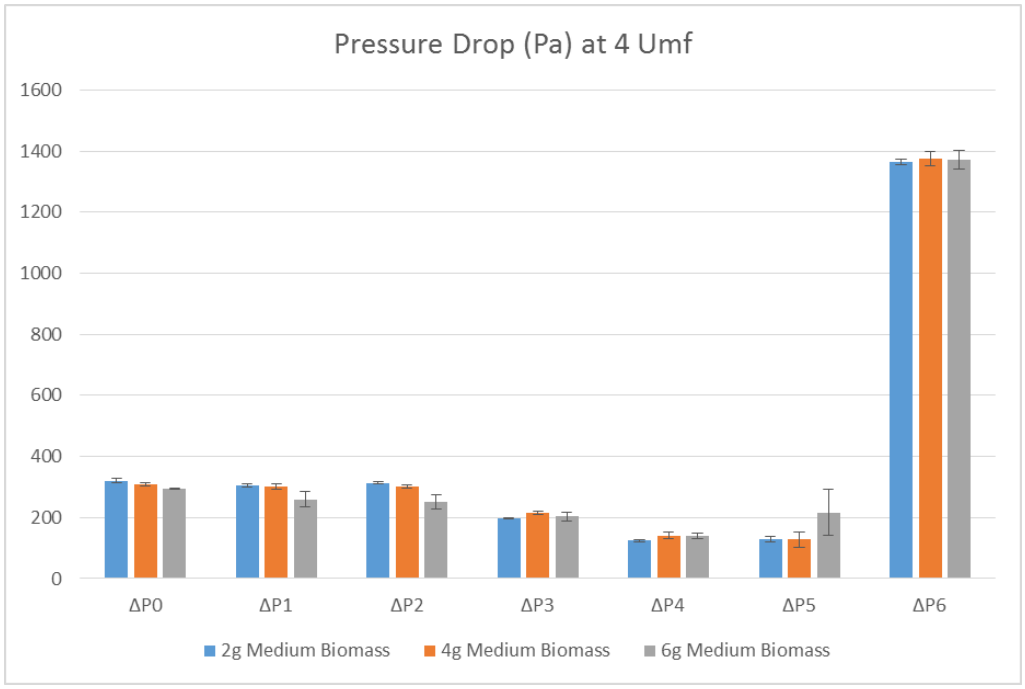

Figure A3: Pressure drop (Pa) for different mass loading of the medium size biomass at a gas velocity of 4 U_{mf}.

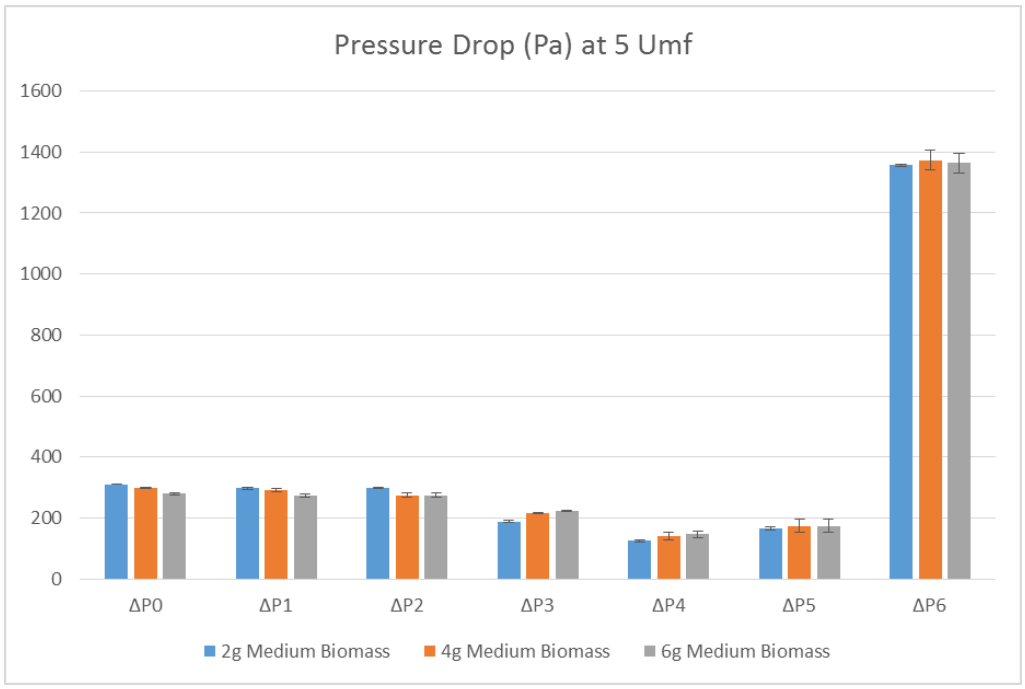

Figure A4: Pressure drop (Pa) for different mass loading of the medium size biomass at a gas velocity of 5 U_{mf}.

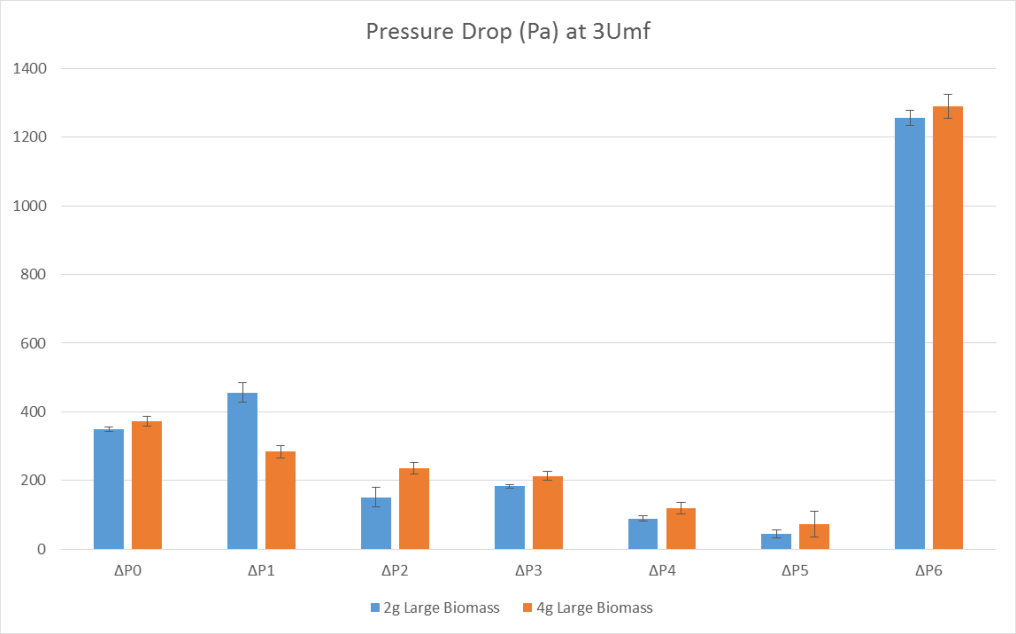

Figure A5: Pressure drop (Pa) for different mass loading of the large size biomass at a gas velocity of 3 U_{mf}.

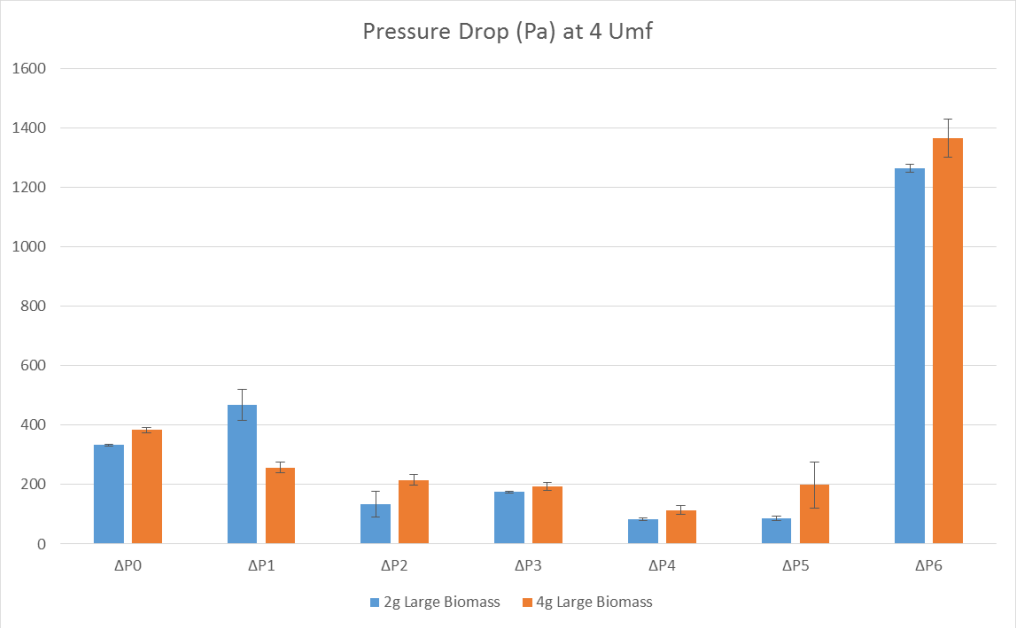

Figure A6: Pressure drop (Pa) for different mass loading of the large size biomass at a gas velocity of 4 U_{mf}.

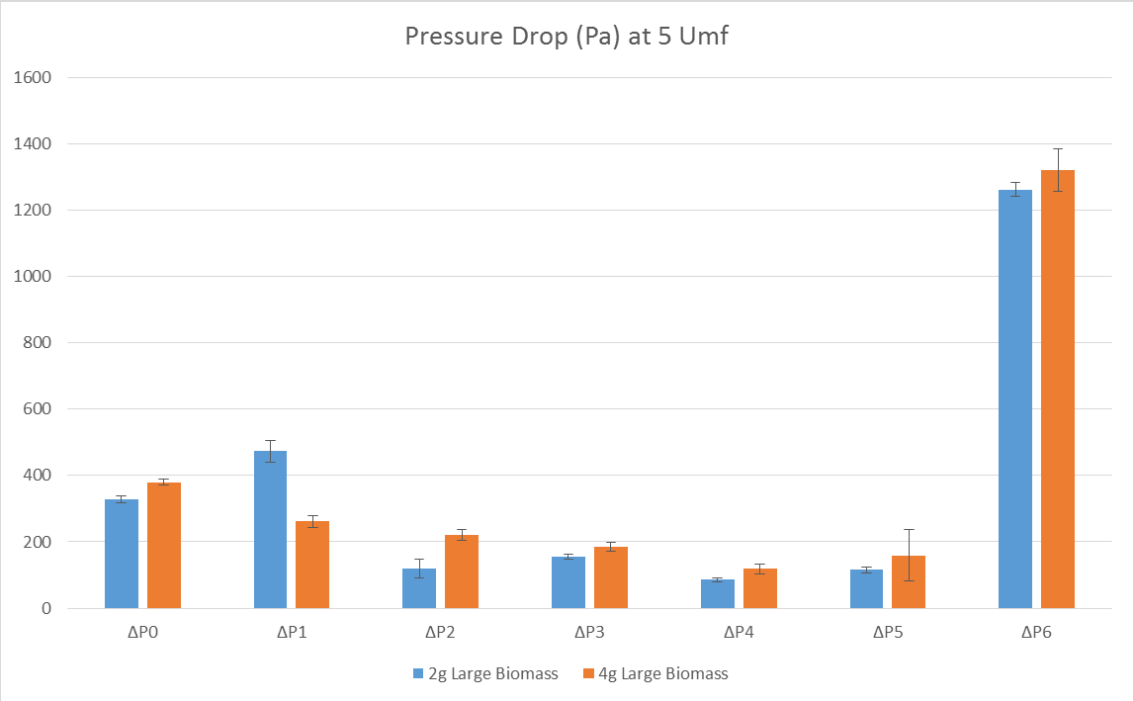

Figure A7: Pressure drop (Pa) for different mass loading of the large size biomass at a gas velocity of 5 U_{mf}.

Brian Anderson, Ph.D.
Director
National Energy Technology Laboratory
U.S. Department of Energy

John Wimer
Associate Director
Strategic Planning
Science & Technology Strategic Plans & Programs
National Energy Technology Laboratory
U.S. Department of Energy

Bryan Morreale
Executive Director
Research & Innovation Center
National Energy Technology Laboratory
U.S. Department of Energy